

## TIMS Pb-Pb geochronology of sulfides in the Fazenda Coqueiro VHMS deposit, São Francisco Craton, NE Brazil: timing and genesis constraints on the Zn-Pb mineralization

*Geocronologia Pb-Pb TIMS de sulfetos do depósito do tipo VHMS da Fazenda Coqueiro, Cráton do São Francisco, NE do Brasil: implicações sobre a idade e a gênese da mineralização de Zn-Pb*

Ricardo Ramos Spreafico<sup>1,2</sup> , Johildo Salomão Figueiredo Barbosa<sup>1,2</sup> ,  
Moacir José Buenano Macambira<sup>3</sup> , Marco Antônio Galarza<sup>3</sup> 

<sup>1</sup>Companhia Baiana de Pesquisa Mineral - CBPM, Centro Administrativo da Bahia, Avenida Quarta, 460, CEP 41745-002, Salvador, BA, BR (spreafico.ricardo@gmail.com; johildo.barbosa@gmail.com)

<sup>2</sup>Universidade Federal da Bahia - UFBA, Instituto de Geociências, Programa de Pós-Graduação em Geologia, Salvador, BA, BA.

<sup>3</sup>Universidade Federal do Pará - UFPA, Instituto de Geociências, Laboratório de Geologia Isotópica, Belém, PA, BR (moamac@ufpa.br; antogt@ufpa.br)

Received on July 27, 2019; accepted on July 20, 2020

### Abstract

TIMS Pb-Pb geochronological data allow determination of the timing and genesis of the Fazenda Coqueiro volcanic-hosted massive sulfide (VHMS) Zn-Pb deposit hosted in the Neoproterozoic Mundo Novo greenstone belt (MNGB), NE São Francisco Craton. The deposit is inserted in the Rhyacian-Orosirian Contendas-Jacobina lineament between Archean cratonic blocks. The basement of the deposit is composed of Paleoproterozoic metagranite and metarhyolite nuclei tectonically emplaced within the supracrustal rocks. The volcanic-sedimentary rocks comprise the ocean floor western metabasalt, calc-silicate rock, aluminous schist, metachert, banded iron formation, and tremolite of the middle sequence and metasedimentary siliciclastic rocks of the uppermost sequence of the MNGB. The western metabasalt is hydrothermally altered, which resulted in the formation of two alteration zones. They consist of carbonate zone, proximal, hosting massive sulfides composed mainly of sphalerite and galena with minor chalcopyrite; and sericite-chlorite zone, distal, hosting mainly disseminated chalcopyrite. Pb-Pb galena, chalcopyrite and sphalerite data from the massive and disseminated zones in the Fazenda Coqueiro deposit yielded model ages of  $2,804 \pm 11.15$ ,  $2,794 \pm 11.2$ , and  $2,767 \pm 11.1$  Ma, respectively, with the Pb sourced from the upper crust, based on the uranium and thorogenic diagrams. The Pb-Pb isochron mineralization age of  $2,747 \pm 16$  Ma obtained from chalcopyrite and sphalerite samples from the massive and disseminated zones suggests that the sulfides were coeval and do not record later metamorphic-hydrothermal events. Therefore, the Fazenda Coqueiro deposit would have formed from Neoproterozoic ocean floor volcanic-exhalative processes. The Rhyacian-Orosirian tectonic event compressed the deposit between Archean blocks along the Contendas-Jacobina lineament, preserving the sulfides from remobilization processes.

**Keywords:** Fazenda Coqueiro Zn-Pb deposit; Pb-Pb geochronology; Neoproterozoic; Volcanic-hosted massive sulfide; Cogenetic sulfides; São Francisco Craton.

### Resumo

Dados geocronológicos TIMS Pb-Pb permitiram determinar o tempo e a gênese do depósito de Zn-Pb *volcanic-hosted massive sulfide* (VHMS) da Fazenda Coqueiro, hospedado no *greenstone belt* Mundo Novo (GBMN) e inserido no lineamento Riáciano-Orosiriano Contendas-Jacobina, NE do Cráton do São Francisco. O seu embasamento é composto por núcleos metagraníticos e metariolíticos Paleoproterozoicos, tectonicamente colocados entre as rochas supracrustais. As rochas vulcanossedimentares de fundo oceânico compreendem metabasalto oeste, calciossilicática, xisto aluminoso, metachert, formação ferrífera bandada e tremolito da sequência média e rochas metassedimentares siliciclásticas da sequência superior do GBMN. O metabasalto oeste hospeda duas zonas de alteração hidrotermal: uma carbonática, proximal, hospedeira do sulfeto maciço e composta de esfalerita e galena, além de menores concentrações de calcopirita; e outra sericítica-clorítica,

distal, que hospeda principalmente calcopirita disseminada. Dados Pb-Pb em galena, calcopirita e esfalerita das zonas maciça e disseminada determinaram idades modelo de  $2.804 \pm 11,15$ ,  $2.794 \pm 11,2$  e  $2.767 \pm 11,1$  Ma, respectivamente, e o chumbo contido nos sulfetos teria como fonte a crosta superior, com base nos diagramas uranogênico e torogênico. Uma idade de mineralização isocrônica de  $2.747 \pm 16$  Ma, obtida de amostras de calcopirita e esfalerita das zonas maciça e disseminada, sugere que os sulfetos sejam cogenéticos e que não registram eventos metamórfico-hidrotermais posteriores. Portanto, o depósito da Fazenda Coqueiro teria se formado a partir de processos vulcano-exalativos de fundo oceânico no Neoarqueano. O evento tectônico Riacciano-Orosiriano comprimiu o depósito entre blocos Arqueanos ao longo do lineamento Contendas-Jacobina, preservando os sulfetos de processos de remobilização.

**Palavras-chave:** Depósito de Zn-Pb Fazenda Coqueiro; Geocronologia Pb-Pb; Neoarqueano; *Volcanic-hosted massive sulfide*; Sulfetos cogenéticos; Cráton do São Francisco.

## INTRODUCTION

The Fazenda Coqueiro volcanic-hosted massive sulfide (VHMS) Zn-Pb deposit, which is hosted in the Mundo Novo greenstone belt (MNGB), in the eastern São Francisco Craton in NE Brazil (Figures 1A, 1B and 1C), records evidence of hydrothermal activity coeval to sulfide precipitation during ocean floor volcanic-exhalative processes in the greenstone terrain.

The VHMS deposit is hosted in the western metabasalt of the middle sequence of the MNGB, which is interlayered with two hydrothermal alteration zones that control sulfide distribution. The carbonate zone is the main portion of the deposit and hosts massive sphalerite and galena occurrences, and the sericite-chlorite zone is peripheral and hosts disseminated chalcopyrite (Spreafico, 2017). A Rhyacian-Orosirian tectonic event (Leite, 2002) deformed the Fazenda Coqueiro deposit during the formation of the Contendas-Jacobina lineament (Barbosa and Sabaté, 2002, 2003, 2004). This event obliterated the initial features of the deposit, making it difficult to interpret the metallogenic model. In this regard, the interpretation of post-hydrothermal processes in the study area would remain possible. In addition, new geochronological data from metavolcanic felsic rock of the MNGB show its Neoproterozoic age (Spreafico et al., 2019), indicating that the Fazenda Coqueiro deposit should be coeval with the volcanic rocks.

However, the deformation during collisional tectonic events, the great depth of the deposit, and the sulfide occurrences identified only in drill cores make it difficult to clearly define the characteristics of the deposit, such as observed by Souza et al. (2002) and Monteiro et al. (2009). Therefore, geological and thermal ionization mass spectrometry (TIMS) Pb-Pb geochronological studies on sulfides from the Fazenda Coqueiro deposit were conducted to more accurately understand and interpret the genesis and timing of the VHMS deposit. The styles, controls, and sources of mineralization, the absence of melt on sulfides during the Rhyacian-Orosirian metamorphic and deformational processes and the relation of the Fazenda Coqueiro deposit with the Contendas-Jacobina lineament were also

covered. The study also aimed to contribute to better establish the prospecting guides on the MNGB and adjoining areas.

## GEOLOGICAL SETTING

The eastern portion of the São Francisco Craton, where the MNGB and the Fazenda Coqueiro deposit are situated (NE Bahia), was formed through the amalgamation of four Archean blocks during Paleoproterozoic continent-continent collisions (Barbosa and Sabaté, 2002, 2003, 2004): the Gavião, Serrinha and Jequié blocks and the Itabuna-Salvador-Curaçá Belt (Figure 1C). The Paleoproterozoic event captured the MNGB and surrounding crust between the cratonic blocks, resulting in the formation of the Contendas-Jacobina lineament. The uplift caused by this event possibly resulted in the erosion and formation of Paleoproterozoic sedimentary basins, such as the uppermost sequence of the MNGB.

Briefly, the MNGB is in contact to the west with 3.4 Ga (Mougeot, 1996) tonalite-trondhjemite-granodiorite (TTG) basement rocks and subordinate metagranites in the Gavião Block and to the east and south with paragneisses in the Saúde Complex with maximum ages between 2.20 and 2.06 Ga (Zincone et al., 2017) (Figure 2). To the north and northwest, the MNGB is in contact with quartzites of the Jacobina Group, which were deposited between 3.55 and 3.22 Ga (Teles et al., 2015) and Paleoproterozoic granitic intrusives.

Additionally, the geological setting includes granulites (2.9 Ga) and multiple charnockite intrusions (2.7 and 2.6 Ga) in the Jequié Block (Wilson, 1987; Silva et al., 2002), tonalitic granulite (2.57 Ga) and enderbite (2.7 Ga) of the Itabuna-Salvador-Curaçá Belt (Silva et al., 1997; Oliveira et al., 2010), and the Mairi (3.33 – 3.30 Ga) and Serrinha (3.1 – 2.9 Ga) blocks (Oliveira et al., 2002a, 2002b; Rios et al., 2009; Sousa et al., 2018) (Figure 1C and Table 1). Although the Itabuna-Salvador-Curaçá Belt and Serrinha Block are far from the MNGB, they are important for understanding the tectonic evolution of the study area.

The eastern margin of the Gavião Block is in tectonic contact with the MNGB along a north-south-trending thrust

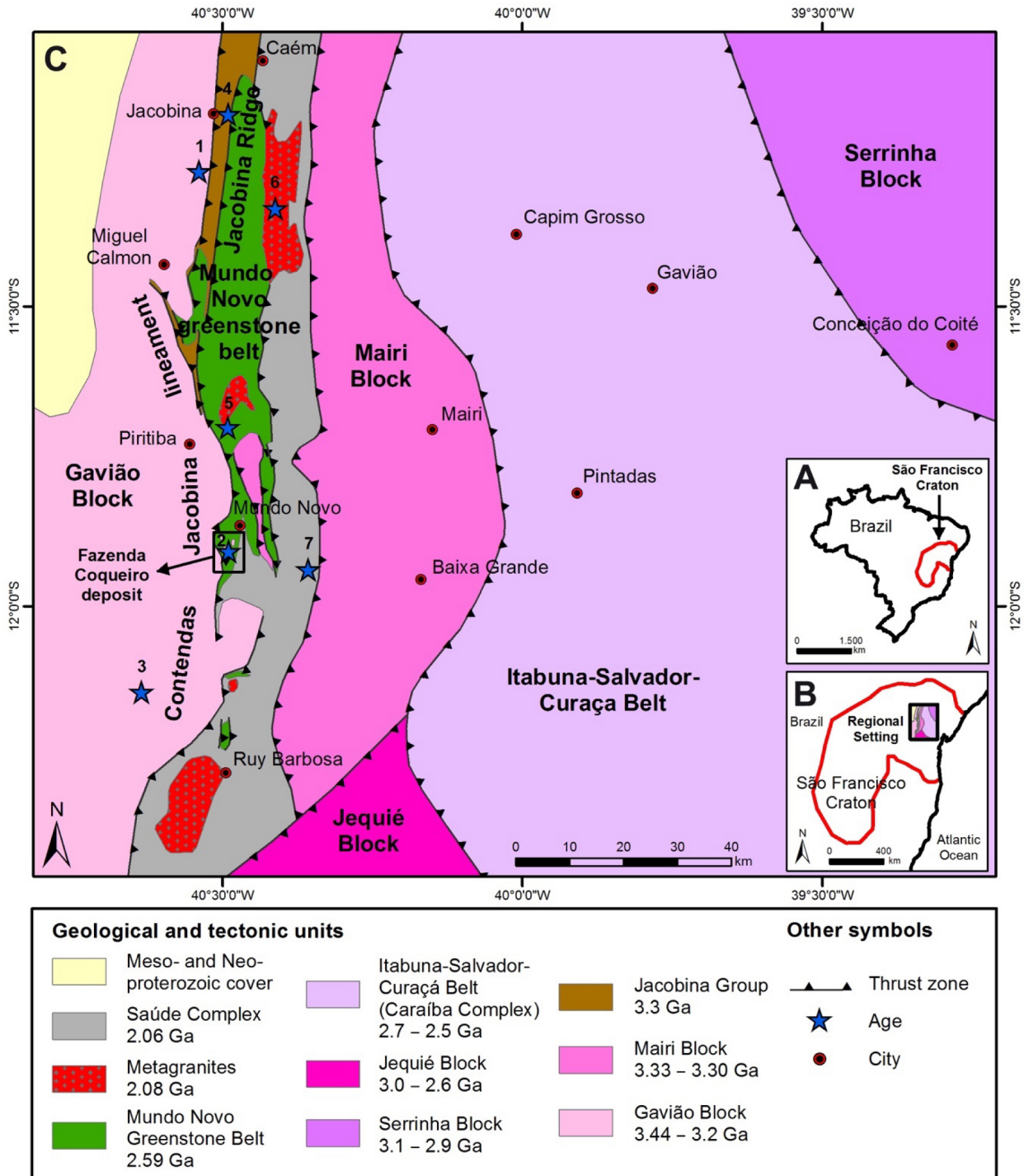


**Figure 1.** (A) Location of the São Francisco Craton in NE Brazil. (B) Regional setting in the eastern portion of the São Francisco Craton. (C) Regional tectonic setting where the Mundo Novo greenstone belt (MNGB) and the Fazenda Coqueiro deposit are inserted (modified from Barbosa and Sabaté, 2002, 2003, 2004). Ages at the points highlighted on the map: (1)  $3,442 \pm 2$  Ma (U-Pb zircon, TTG; Mougeot, 1996); (2)  $3,303 \pm 11$  Ma (U-Pb zircon, metarhyolite from the Gavião Block obtained by Zincone et al., 2016); (3)  $3,292 \pm 3$  Ma (U-Pb zircon, metagranite from the Gavião Block obtained by Zincone et al., 2016); (4)  $3,500\text{--}3,220$  Ma (U-Pb zircon, quartzite from the Jacobina Group obtained by Teles et al., 2015); (5)  $2,595 \pm 21$  Ma (U-Pb zircon, metadacite from the MNGB obtained by Spreafico et al., 2019); (6)  $2,080 \pm 18$  Ma (U-Pb monazite, Cachoeira Grande granite obtained by Leite, 2002); (7)  $2,068 \pm 12$  Ma (U-Pb zircon, biotite schist from the Saúde Complex obtained by Zincone et al., 2017).

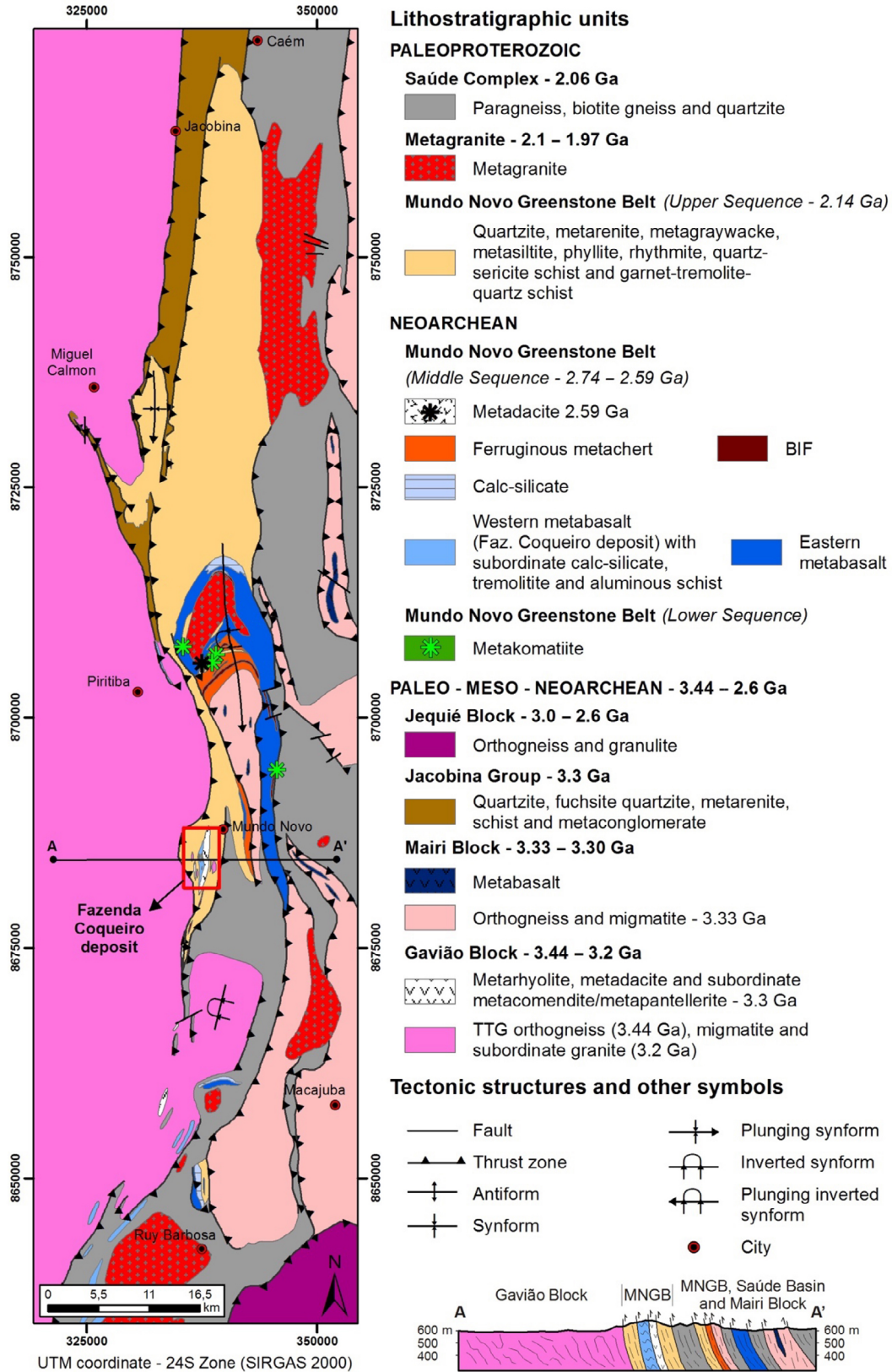


**Figure 2.** Geological map of the Mundo Novo greenstone belt and adjoining units. From Spreafico et al. (2019) and updated with data from the present work.

**Table 1.** Compilation of regional geochronological data from the Mundo Novo greenstone belt and adjoining units.

Geological/ tectonic unit	Lithotype	Age	Method	Mineral dated	Author
Saúde Complex	Biotite schist	2068 ± 12 Ma	U-Pb (LA-MC-ICP-MS)	Detrital zircon	Zincone et al. (2017)
Cachoeira Grande granite	Leucogranite	2080 ± 18 Ma	U-Pb (electron microprobe)	Monazite (crystallization age)	Leite (2002)
Upper sequence (MNGB)	Quartzite	2133 ± 14 Ma	U-Pb (LA-ICP-MS)	Detrital zircon	Barbuena et al. (2016)
Mundo Novo greenstone belt (metavolcanic rocks)	Metadacite	2595 ± 21 Ma	U-Pb (LA-ICP-MS)	Zircon (crystallization age)	Spreafico et al. (2019)
Itabuna-Salvador-Curaçá Belt	Tonalitic granulite	2574 ± 6 Ma	U-Pb (SHRIMP)	Zircon (crystallization age)	Oliveira et al. (2010)
	Enderbite	2695 ± 12 Ma	U-Pb (SHRIMP)	Zircon (crystallization age)	Silva et al. (1997)
Jequié Block	Granulites	2715 ± 29 Ma	U-Pb (SHRIMP)	Zircon (crystallization age)	Silva et al. (2002)
	Charnockite	2900 ± 24 Ma	Rb-Sr	Whole-rock (crystallization age)	Wilson (1987)
Serrinha Block	Granitoid	2989 ± 11 Ma 3072 ± 2 Ma 3162 ± 26 Ma	U-Pb (SHRIMP)	Zircon (crystallization age)	Rios et al. (2009)
	Gneiss, migmatite	3152 ± 5 Ma	U-Pb (SHRIMP)	Zircon (crystallization age)	Oliveira et al. (2002a, 2002b) Magee et al. (2001); Teles (2013); Teles et al. (2015); Barbuena et al. (2016)
Jacobina Group	Quartzite	3500 – 3220 Ma	U-Pb (LA-MC-ICP-MS)	Detrital zircon	Teles et al. (2015); Barbuena et al. (2016)
Mairi Block	Orthogneiss	3.33 – 3.30 Ga	U-Pb (LA-SF-ICP-MS)	Zircon (crystallization age)	Sousa et al. (2018)
	Metagranite	3291 ± 2.5 Ma	U-Pb (LA-ICP-MS)	Zircon (crystallization age)	Zincone et al. (2016)
Gavião Block	Metarhyolite*	3303 ± 11 Ma	U-Pb (LA-ICP-MS and SHRIMP)	Zircon (crystallization age)	Peucat et al. (2002); Zincone et al. (2016)
	TTG	3442 ± 2 Ma	U-Pb (ID-TIMS)	Zircon (crystallization age)	Mougeot (1996)

MNGB: Mundo Novo greenstone belt; TTG: tonalite-trondhjemite-granodiorite; U-Pb: uranium-lead; LA-MC-ICP-MS: laser ablation multi-collector inductively coupled plasma mass spectrometry; SHRIMP: sensitive high-resolution ion microprobe; ID-TIMS: isotope dilution thermal ionization mass spectrometry; \*the metarhyolite with an age of 3,303 ± 11 Ma is part of the basement (Gavião Block) of the Fazenda Coqueiro deposit; LA-SF-ICP-MS: laser ablation sector field inductively coupled plasma mass spectrometry.

zone with a west vergence (Figure 1C) and is composed of TTG gneisses and migmatites that host mafic rock enclaves (Barbosa et al., 2012a), metagranites, and metarhyolites (Peucat et al., 2002; Zincone et al., 2016). This block corresponds to the basement of the MNGB. Three groups of TTG gneisses are described in the Gavião Block; two groups are trondhjemitic with U-Pb zircon ages (sensitive high-resolution ion microprobe – SHRIMP) of 3,403 ± 5 and 3,158 ± 5 Ma

(Barbosa, 1997; Leal, 1998), and the third group, of granodioritic composition, includes the 3,225 ± 10 Ma Aracatu granitoid (Barbosa et al., 2012a). The age of the Gavião Block is 3.4 Ga (Mougeot, 1996), but metarhyolites with ages of 3,303 ± 11 Ma and metagranites, such as Boa Sorte at 3,291 ± 2.5 Ma, occur as well (Zincone et al., 2016).

The Jacobina Group is in tectonic contact with the MNGB along thrust zones, all of which strike north-south and are

vergent to the west (Figure 1C), with the Gavião Block in the footwall. The Jacobina Group comprises metaconglomerates, quartzites, metarenites, phyllites, chlorite schists, and quartz-sericite schists (Mascarenhas et al., 1998) deposited in a passive margin setting (Reis et al., 2018). This group has a depositional age, based on detrital zircons, between 3,500 and 3,220 Ma (Magee et al., 2001; Teles, 2013; Teles et al., 2015; Barbuena et al., 2016). Jacobina Ridge represents an Archean supracrustal sequence with a maximum depositional age of 3.22 Ga, and its sources are likely rocks from both the plutonic-volcanic system and the TTG suite in the Gavião Block (Zinconone et al., 2016).

The MNGB is divided into three stratigraphic sequences (Spreafico et al., 2019): a lowermost sequence (ultramafic rocks), a middle sequence (mafic and felsic igneous rocks and clastic and chemical metasedimentary rocks) and an uppermost one composed of siliciclastic metasedimentary rocks with an inherited zircon age of  $2,133 \pm 14$  Ma (Barbuena et al., 2016) (Figure 2). Two ductile and progressive Paleoproterozoic deformational phases are described in the MNGB. The  $D_1$  deformational phase is characterized by isoclinal and recumbent folds vergent to the west that generated greenschist-facies metamorphic rocks. The  $D_2$  deformational phase is characterized by refolding the vertical and subvertical axial planes and eventually resulted in the formation of coaxial interference patterns or compressive and transpressive shear zones, which bounded the MNGB lithotypes and generated rocks of greenschist- to amphibolite-facies metamorphism. The most prominent brittle structures are east-trending faults and fractures. The Neoproterozoic volcanism in the MNGB (Spreafico et al., 2019) and the Paleoproterozoic sedimentation at the top of the sequence (Barbuena et al., 2016) coeval to the Paleoproterozoic tectonic event (Leite, 2002) have been considered the main geological and tectonic events in the study area.

As far as the Fazenda Coqueiro deposit is concerned, drill hole programs previously carried out by *Companhia Baiana de Pesquisa Mineral* (CBPM) quantified resources of 4,200,000 t in the massive sulfide body at 6.12% Zn and 0.41% Pb and a one-meter thick intersection that reached 28 g/t Ag content (Monteiro et al., 2009). Gold occurrences related to the massive sulfides reached 2.75 g/t in a two-meter thick intersection, and one Cu-rich disseminated zone in a four-meter thick intersection reached 0.75% average Cu content (Monteiro et al., 2009).

The Saúde Complex occurs to the east of the MNGB (Figure 1C), where the two units are in tectonic contact along west-vergent thrust zones, and is distributed along the Contendas-Jacobina lineament. The Saúde Complex comprises aluminous paragneisses, biotite gneisses, and subordinate quartzites widely distributed in a north-south trend with significant occurrences in the Mundo Novo region

and in the eastern portion of Jacobina Ridge (Couto et al., 1978; Mascarenhas et al., 1998; Leite et al., 2007; Reis et al., 2017) (Figure 1C). The maximum depositional age of 2.06 Ga (Zinconone et al., 2017) for the Saúde Complex once more indicates the presence of a basin near the MNGB in the Paleoproterozoic that was later subjected to a high-grade metamorphic process.

Paleoproterozoic granites are present along the Contendas-Jacobina lineament (Figure 1C) (Leite, 2002). In general, these granites are undeformed leucogranites that comprise quartz, feldspar, biotite, and muscovite, with occurrences of garnet and sillimanite (Barbosa et al., 2012b). The Cachoeira Grande granite, for example, is a peraluminous leucogranite situated to the northeast of the MNGB that has an average age of  $2,080 \pm 18$  Ma (Leite, 2002), coeval with the Rhyacian-Orosirian granitic intrusions in the MNGB.

## ANALYTICAL METHODOLOGY

The Fazenda Coqueiro deposit study involved the geological description of cores of five drill holes acquired by CBPM (Figure 3) in the 1990s, including petrographic analyses, and the collection of sulfides and hydrothermal alteration samples from three of these drill holes for timing and genesis constraints in mineralization.

The description of drill cores was represented in a geological and structural section and in a diagram block, where the hydrothermal alteration zones were represented and the locations of collected samples for geochronological study were indicated.

For petrographic studies of thin sections and polished thin sections, the mineralogical composition and microstructures of the rocks were determined using the ZEISS Axio Scope.A1 microscope, provided by CBPM. The mineral abbreviations used in petrographic images and other figures throughout the manuscript follow those of Kretz (1983) and Siivola and Schmid (2007).

To better illustrate the mineral paragenesis of the host rocks, we used backscattered electron images of polished thin sections from a Kevex energy dispersive spectroscopy (EDS) in a CAMECA SX50 electron microprobe at the Universidade de Brasília. The standards used were synthetic with defined compositions, such as AsGa (for As), ZnS (for Zn), PbS (for Pb), FeS<sub>2</sub> (for Fe), CuFeS<sub>2</sub> (for Cu), and the standard Ni for the homonymous element.

With regard to geochronology, twelve samples of sulfides from the Fazenda Coqueiro deposit were selected to determine their model and crystallization ages using the Pb-Pb method on sulfides. Pb-Pb geochronology was carried out at the Isotope Geology Laboratory of the Institute of Geosciences, Universidade Federal do Pará. Sulfide grains from each sample were separated using binocular

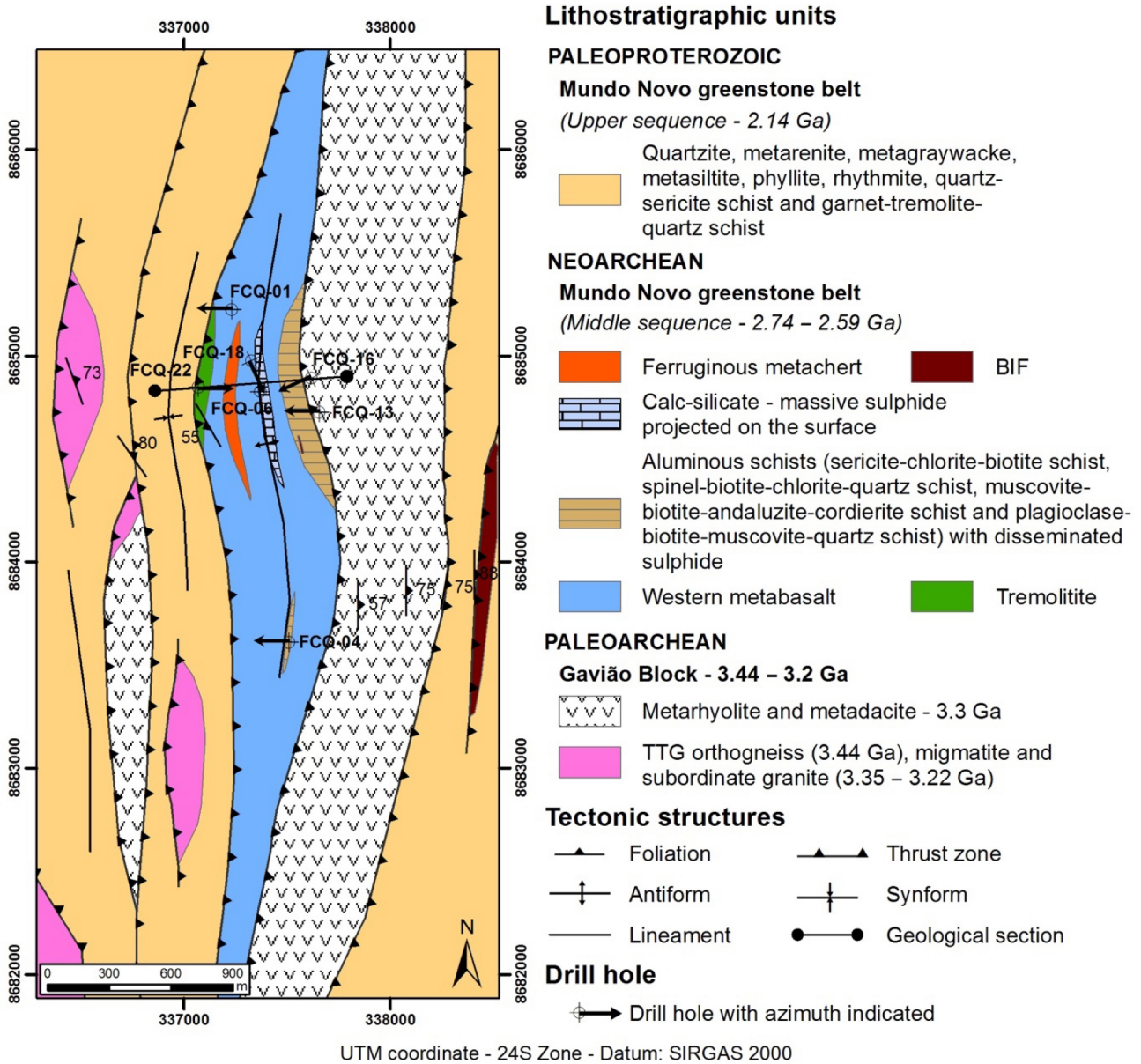


**Figure 3.** Geological map of the Fazenda Coqueiro volcanic-hosted massive sulfide deposit and the drill hole sites where the sulfide samples were collected for Pb-Pb analyses.

microscopy. To determine the Pb isotope compositions from galena, sphalerite, and chalcopyrite, three different techniques were applied: whole digestion, leached fractions, and galena analysis. Before acid digestion, 100 µg samples were cleaned, alternating among deionized H<sub>2</sub>O (three times), 1 ml HCl 6N (50°C, five minutes) and five minutes in ultrasound (twice). For whole digestion, 2 mL of a 6N HCl + HNO<sub>3</sub> cc (1:1) solution plus 1 drop of 8N HBr were introduced twice in the sample, left for twenty-four and six hours,

separated by five minutes of ultrasound and finally evaporated. For leaching fractions, a solution of 4 mL of 4N HBr + 2N HCl (12:1) was introduced into the sample and left for fifteen minutes at 110°C. Subsequently, the supernatant was collected and evaporated. The residue was evaporated, and 4 ml of 2N HBr were introduced and left for four hours at 110°C. The procedure was repeated, but the acid solution was changed to 4 mL of 4N HCl for twelve hours at 110°C; 4 mL of 6N HCl for six hours at 110°C; and 4 mL of 50%

aqua regia for twenty-four hours at 110°C until the whole sample was consumed, which generated a maximum of five leaching fractions. For the galena digestion, three drops of 8N HBr were introduced into the sample and evaporated, followed by 2 mL of 13N HNO<sub>3</sub> and evaporation; another 2 mL of 13N HNO<sub>3</sub> plus 4 ml of deionized H<sub>2</sub>O were added, and finally, 20 µL of H<sub>3</sub>PO<sub>4</sub> (0.125M) were introduced, and the solution was evaporated. Except for the galena solution, the others were processed in a chromatographic separation column filled with Dowex AG 1 × 8 resin in the following sequence: cleaning of the resin (6N HCl, deionized H<sub>2</sub>O, 0.5N HBr twice), introduction of the sample solution into the column, and elution four times with 0.5N HBr; finally, the Pb was recovered with 6N HCl. Before evaporation, 10 µL of 0.125N H<sub>3</sub>PO<sub>4</sub> were introduced for analysis on a Finnigan Mat 262 TIMS. The final results were plotted in the Pb-Pb diagrams for model and isochron age determination, as well as plumbotectonic models, using the Isoplot Excel program.

## RESULTS

### Geology of the Fazenda Coqueiro volcanic-hosted massive sulfide deposit

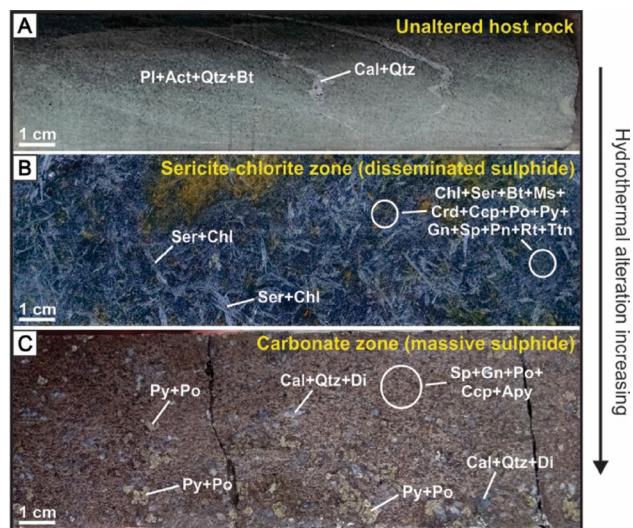
The MNGB is divided into three stratigraphic sequences as follows: the lowermost sequence, composed of meta-komatite; the middle sequence, composed of western and eastern metabasalts and subordinate tremolite, calc-silicate rock, aluminous schist, banded iron formation, ferruginous metachert, basaltic metandesite, metadacite and metarhyolite; and the uppermost sequence, composed of siliciclastic metasedimentary rocks, such as metarenites, quartzites, metagraywackes, metasiltites, phyllites, rhythmities, quartz-sericite schists, and garnet-tremolite-quartz schists (Spreafico et al., 2019).

In the Fazenda Coqueiro deposit, two supracrustal lithological sequences of the MNGB are present and tectonically related to basement rocks (Figure 3), the middle and uppermost sequences. The Paleoproterozoic metagranite and metarhyolite of the Gavião Block occur as tectonic slices emplaced within the rocks of those sequences. The lithotypes of the middle sequence in the Fazenda Coqueiro deposit consist of the western metabasalt that hosts the mineralization, with calc-silicate and aluminous schist interlayered, in addition to tremolite, ferruginous metachert and banded iron formation. The metasedimentary rocks of the uppermost sequence in the Fazenda Coqueiro deposit comprise mainly metarenites, quartzites, metagraywackes, metasiltites, phyllites, and rhythmities in the eastern and western contacts of the deposit where these rocks can reach three kilometers in thickness.

### Host rock

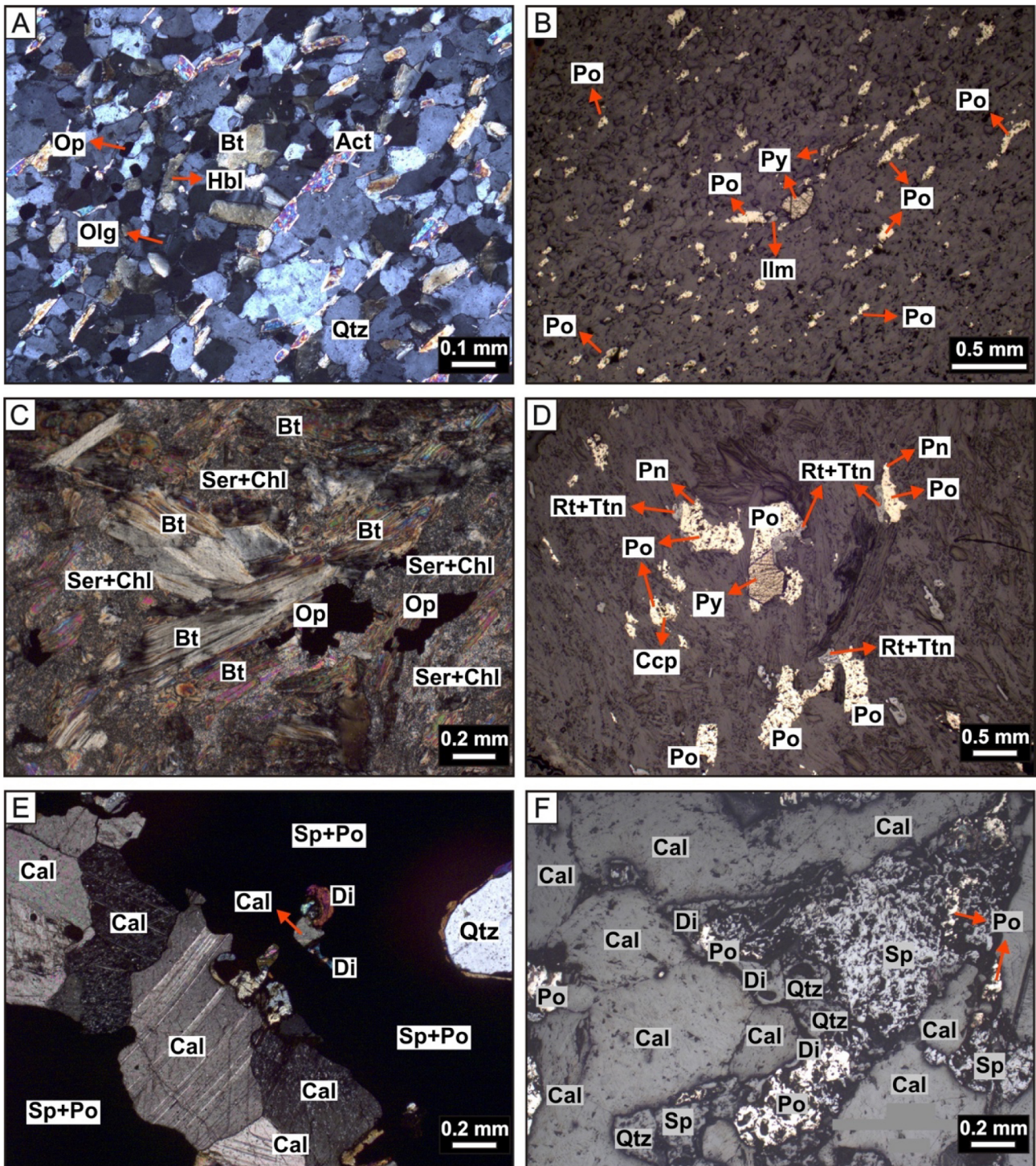
The western metabasalt hosts two distinct metamorphosed hydrothermal alteration zones and is distributed along a north-south trend in the Fazenda Coqueiro deposit (Figure 3). The metabasalt also shows enrichment in light rare earth elements and high intraoceanic crustal input, in addition to an intraoceanic arc-basin geochemical pattern, such as described by Spreafico et al. (2019).

The rock is anisotropic, inequigranular, and aphanitic, has a green to grey color and a polygonal granoblastic microstructure. It is composed of actinolite and oligoclase with low percentages of augite, hornblende, quartz, and biotite, as well as ilmenite and titanite as accessory minerals (Figures 4A and 5A). Intergrowth of pyrrhotite and pyrite (Figure 6A) and trace amounts of chalcopyrite, galena, sphalerite, and arsenopyrite were also described. The biotite and actinolite grains are oriented and define well-developed



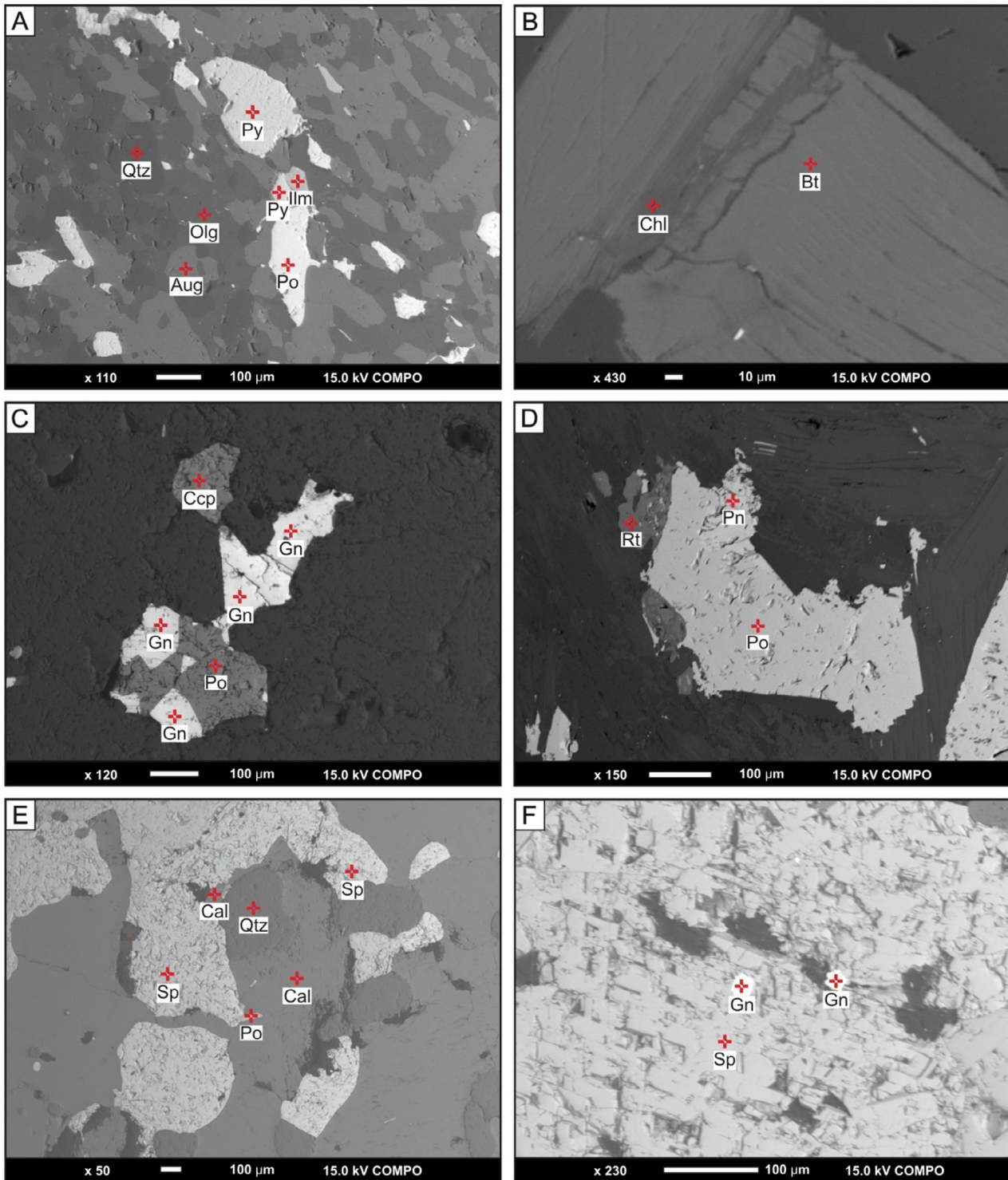
Act: actinolite; Apy: arsenopyrite; Bt: biotite; Cal: calcite; Ccp: chalcopyrite; Chl: chlorite; Crd: cordierite; Di: diopside; Gn: galena; Ms: muscovite; Pl: plagioclase; Pn: pentlandite; Po: pyrrhotite; Py: pyrite; Qtz: quartz; Rt: rutile; Ser: sericite; Sp: sphalerite; Ttn: titanite.

**Figure 4.** Core samples of the host rock and hydrothermal alteration zones in the Fazenda Coqueiro volcanic-hosted massive sulfide (VHMS) deposit with the hydrothermal alteration increasing from the unaltered western metabasalt to the carbonate zone. (A) Unaltered western metabasalt host rock composed of plagioclase, actinolite, quartz, and biotite intersected by calcic-quartz veins. (B) Sericitic-chlorite zone (aluminous schist) composed of sericite, chlorite, biotite, muscovite, and cordierite with disseminated chalcopyrite and traces of pyrrhotite, pyrite, galena, sphalerite, pentlandite, and rutile. (C) Carbonate zone (calc-silicate rock) composed of calcite and quartz with massive sphalerite and traces of galena, pyrrhotite, pyrite, and arsenopyrite.



Act: actinolite; Bt: biotite; Cal: calcite; Ccp: chalcopyrite; Chl: chlorite; Di: diopside; Hbl: hornblende; Ilm: ilmenite; Olg: oligoclase; Op: opaque mineral; Pn: pentlandite; Po: pyrrhotite; Py: pyrite; Qtz: quartz; Rt: rutile; Ser: sericite; Sp: sphalerite; Ttn: titanite.

**Figure 5.** Petrographic images of the western metabasalt and metamorphosed hydrothermal alteration zones. (A) Very fine-grained and polygonal granoblastic microstructure and oriented grains in the western metabasalt (cross polarized light). (B) Traces of elongated and oriented pyrrhotite and pyrite grains in the western metabasalt (reflected light). (C) Sericite-chlorite zone composed of biotite, chlorite, sericite, and opaque minerals (plane polarized light). (D) Elongated and oriented sulfide grains in the sericite-chlorite zone (reflected light). (E) Intergrowth of silicates, carbonate and sulfides in the carbonate zone (cross polarized light). (F) Intergrowth of sphalerite, pyrrhotite, calcite, quartz, and diopside in the carbonate zone (reflected light).



Aug: augite; Bt: biotite; Cal: calcite; Ccp: chalcopryite; Chl: chlorite; Gn: galena; Ilm: ilmenite; Olg: oligoclase; Pn: pentlandite; Po: pyrrhotite; Py: pyrite; Qtz: quartz; Rt: rutile; Sp: sphalerite.

**Figure 6.** Backscattered electron images with the analytical spots in the core samples of the Fazenda Coqueiro volcanic-hosted massive sulfide deposit. (A) Intergrowth of pyrite and pyrrhotite, and very fine-grained and polygonal granonematoblastic microstructure in the western metabasalt. (B) Replacement of chlorite by biotite in the sericite-chlorite zone. (C) Intergrowth of chalcopyrite, galena and pyrrhotite in the silica-rich level in the sericite-chlorite zone. (D) Intergrowth of pyrrhotite, pentlandite and rutile in the sericite-chlorite zone. (E) Intergrowth of sphalerite, pyrrhotite, calcite, and quartz in the carbonate zone. (F) Inclusions of galena in sphalerite grains hosted in the carbonate zone.

planes of foliation, along which the anhedral and partially broken sulfide grains also show a well-defined elongated and oriented pattern (Figure 5B).

The occurrence of the western metabasalt is 500-meter thick and 5 to 6-kilometer long in the deposit and comprises the hanging wall of the massive sulfide level (Figure 7). It makes tectonic contact along thrust zones with metarhyolites of the basement to the east and with siliciclastic metasedimentary rocks to the west (Figure 3).

Two metamorphosed hydrothermal alteration zones occur interlayered with the western metabasalt. One of them is a proximal carbonate zone that hosts massive sulfides in the Fazenda Coqueiro deposit, composed mainly of sphalerite and galena; and the other is a distal sericite-chlorite zone that hosts disseminated sulfides composed mainly of chalcopyrite.

#### *Sericite-chlorite zone*

The sericite-chlorite zone is distal and observable mainly in drill cores (Figure 4B). This zone is interlayered with the western metabasalt at different levels and comprises the footwall of the massive sulfide level (Figures 7 and 8).

This sericite-chlorite zone hosts disseminated and lower sulfide content with a predominance of chalcopyrite. The main rock that composes this zone is the sericite-chlorite-biotite schist, which shows replacement features of chlorite by biotite (Figures 5C and 6B). Other rocks that comprise the sericite-chlorite zone are spinel-biotite-chlorite-quartz schist, muscovite-biotite-andalusite-cordierite schist, and plagioclase-biotite-muscovite-quartz schist. These four rocks are also compositionally termed as aluminous schists.

The anhedral and partially broken chalcopyrite, pyrrhotite and pyrite grains and the traces of rutile and titanite are elongated and oriented along the foliation planes and concordant with the phyllosilicates (Figure 5D). The paragenesis also involves intergrowth of galena, chalcopyrite, and pyrrhotite within a thin silica-rich level that occurs between the sericite-chlorite and the carbonate zone (Figure 6C), and intergrowth of galena, pentlandite and sphalerite in the sericite-chlorite zone (Figure 6D).

#### *Carbonate zone*

The carbonate zone is proximal and hosts massive and higher content sulfides that are strata-bound and composed

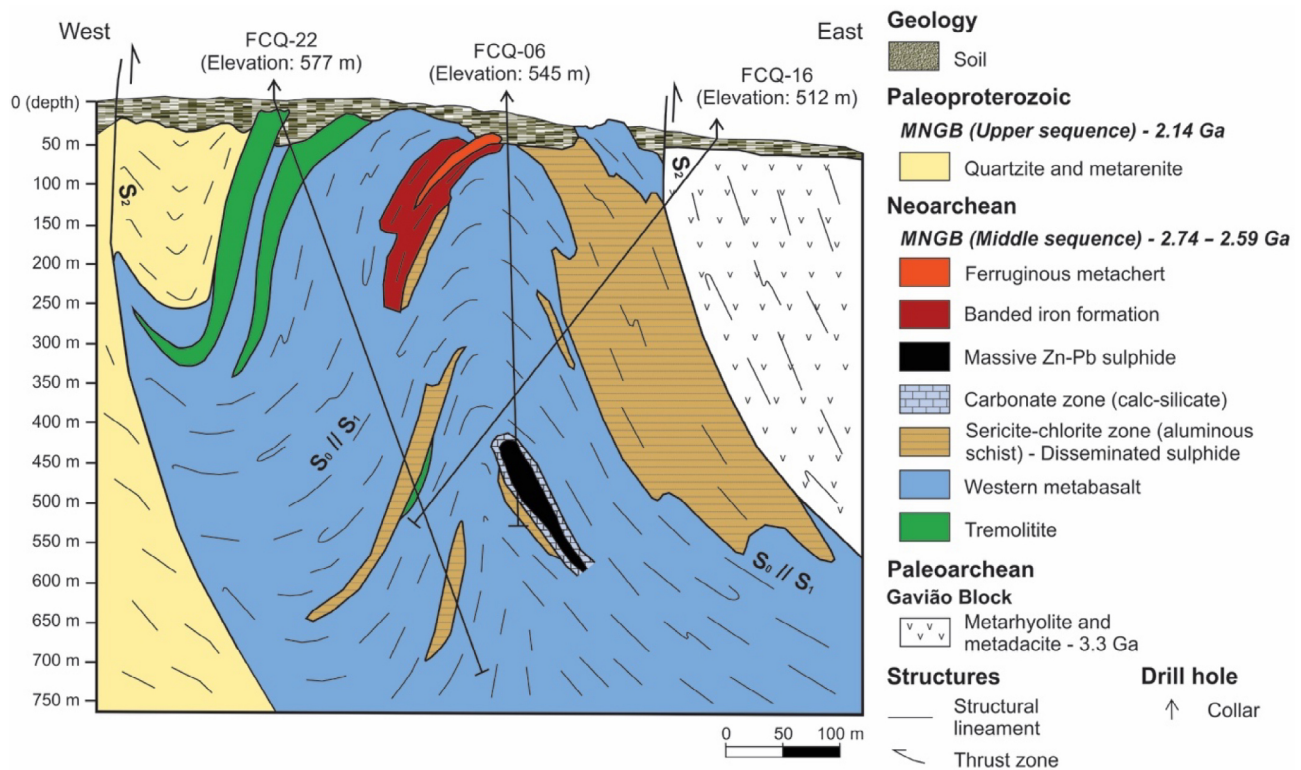


**Figure 7.** Geological cross section of the Fazenda Coqueiro volcanic-hosted massive sulfide deposit showing the antiform, the distribution of the western metabasalt, and the carbonate and sericite-chlorite zones based on outcrops and drill core descriptions. The site of the geological cross section is represented in the geological map of Figure 3.

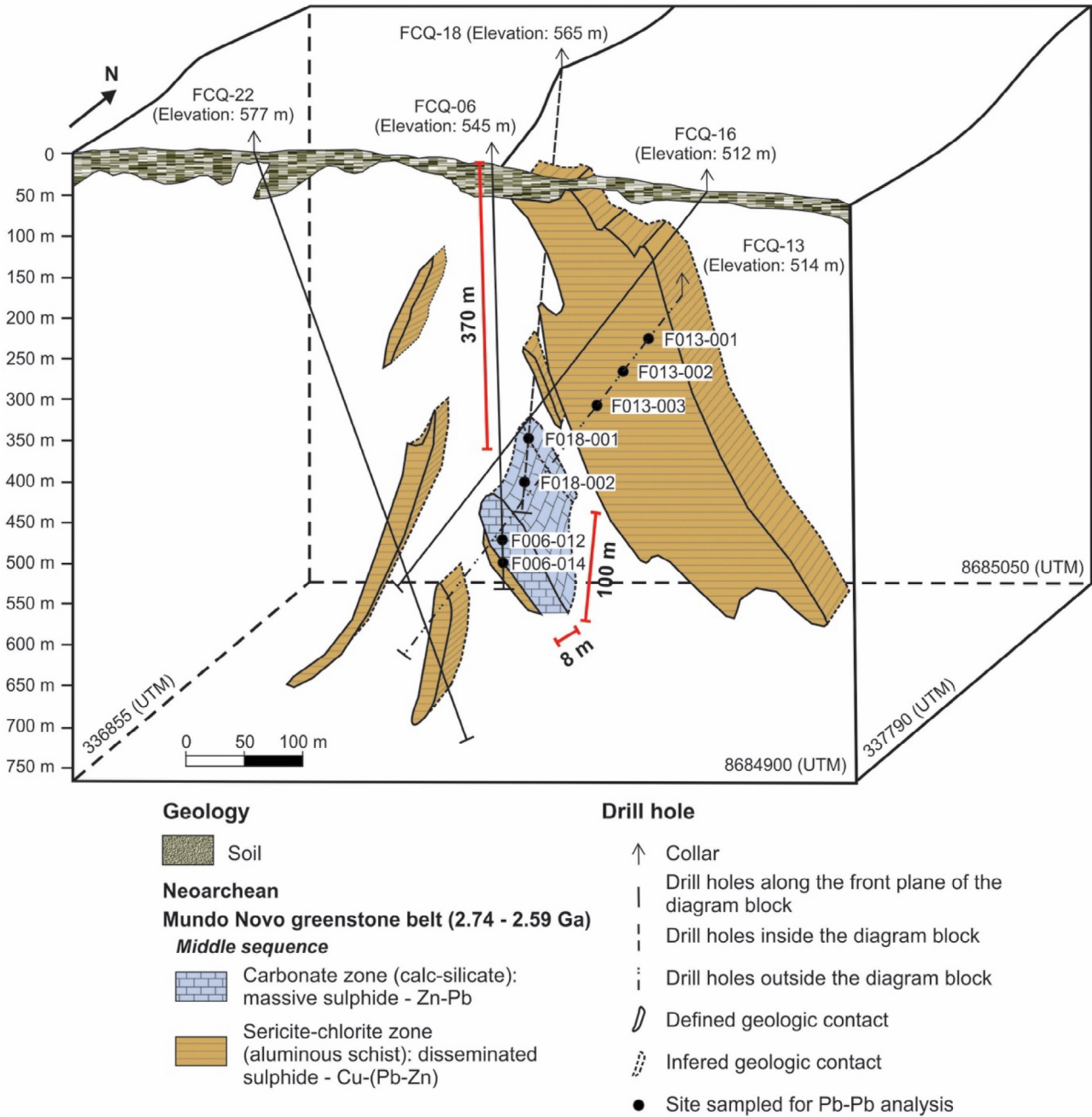


**Figure 8.** Block diagram of the Fazenda Coqueiro volcanic-hosted massive sulfide deposit showing the distribution and geometry interpreted for metamorphosed hydrothermal alteration zones, the associated mineralization and the sites sampled for Pb-Pb analysis. See Appendix 1 for collar coordinates.

mainly of sphalerite with a minor amount of galena and traces of chalcopyrite, arsenopyrite, pyrrhotite, and pyrite (Figure 4C). The carbonate zone is also composed of intergrowths of anhedral calcite, quartz, and diopside grains that coexist with the sulfides and can be involved

by them (Figures 5E and 6E). The sphalerite grains contain inclusions of galena, show intergrowth with pyrrhotite (Figures 5F and 6F) and are related to restricted occurrences of silver and gold in the massive zone. The metamorphic product of the carbonate alteration zone was

compositionally classified as a calc-silicate rock based on the gangue mineral content.

The carbonate zone forms a subvertical lens in the eastern limb of a tight antiform with a north-south and subhorizontal hinge line plunging southward (Figure 7). The hanging wall is composed of the western metabasalt, and the footwall consists of one level of sericite-chlorite zone, where thin silicate levels can occur with low galena, chalcopyrite, pyrrhotite, and arsenopyrite contents. The carbonate lens is 8-meter thick and at least one hundred meters in length along the north-south direction and with the top at a depth of approximately 370 meters (Figure 8). However, the extent of the massive sulfide lens at greater depths is yet unknown.

### Structural geology

The result of the west vergent Rhyacian-Orosirian tectonic event in the rocks of the Fazenda Coqueiro deposit was a tectonic tightening with slices of the basement metarhyolites emplaced in the supracrustal rocks along thrust zones. Therefore, the metarhyolites overlapped on the western metabasalts of the middle sequence in the eastern part of the deposit, and the western metabasalts overlapped on the metasedimentary siliciclastic rocks of the uppermost sequence in the western part of the deposit (Figure 7).

The antiform outlined by the carbonate and sericite-chlorite zones (Figure 8) encloses the Fazenda Coqueiro deposit and continues to a synform to the west. Like the antiform, the synform also has a north-south hinge line plunging to the south and limbs with high-angle dips and is limited by a west vergent thrust zone.

The  $S_0$  and  $S_1$  structures were parallelized during the first west vergent deformational phase constituting the limbs of the antiform and synform that developed during the second west vergent deformational phase. This second deformational phase produced subvertical axial planes and thrust zones, both interpreted as  $S_2$  structures. The concordance of the massive sulfide lens with the  $S_0$  and  $S_1$  structures and its subvertical position suggests that the massive sulfide zone may also be parallel to the subvertical  $S_2$  structures.

### Pb-Pb geochronology of sulfides

The geochronological study of the Fazenda Coqueiro deposit was focused on galena, chalcopyrite, and sphalerite grains from the western metabasalt (host rock), sericite-chlorite zone (aluminous schist), and carbonate zone (calc-silicate) of the middle sequence of the MNGB.

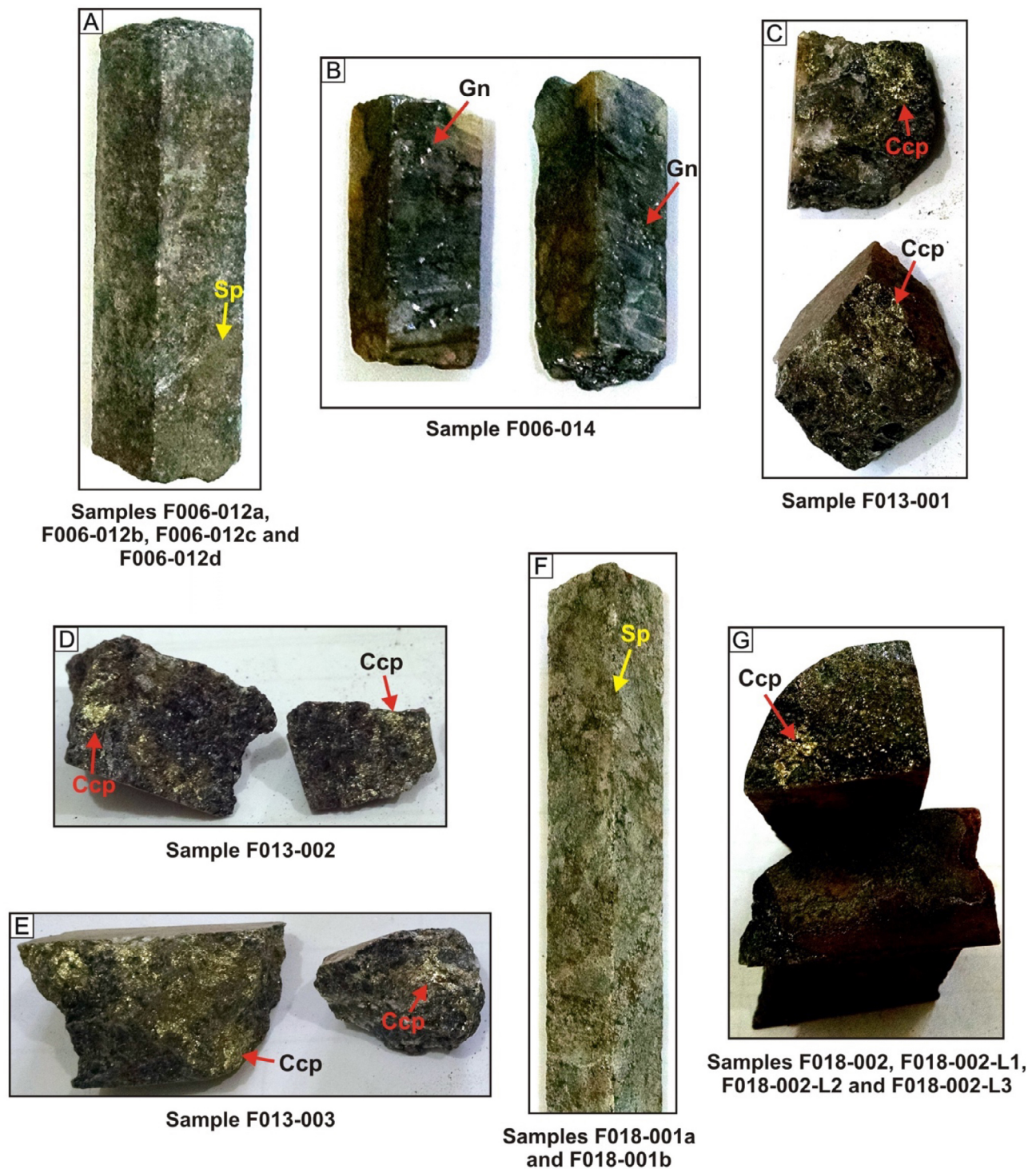
The twelve sulfide samples for Pb-Pb geochronology analysis were collected from cores of three drill holes in the Fazenda Coqueiro deposit: FCQ-06, FCQ-13, and FCQ-18 (Figures 3 and 8). The five samples acquired from drill

hole FCQ-06 are F006-012a, F006-012b, F006-012c, and F006-012d (collected from the carbonate zone), and F006-014 (collected from the silica-rich level). The three samples obtained from drill hole FCQ-13 are F013-001, F013-002, and F013-003 (collected from the sericite-chlorite zone); and the four samples obtained from drill hole FCQ-18 are F018-001a, F018-001b, F018-002, and F018-002-L (collected from the carbonate zone) (Figures 8 and 9). The F018-002L sample generated three more samples through the leached preparation technique, which were used in the tectonic source diagrams. All isotopic results obtained and used for diagram plots are presented in Table 2.

A galena grain sampled from a silica-rich level of the sericite-chlorite zone and sphalerite and chalcopyrite grains sampled from the carbonate zone (massive sulfide) were used to determine the model ages. The similarity of the results obtained for the three samples shows that the model was obeyed, in addition to indicating a unique and isotopically homogeneous source for the three analyzed sulfides. Thus, the galena yields a model age of  $2,804 \pm 11.15$  Ma (Figure 10A), the chalcopyrite yields a model age of  $2,794 \pm 11.2$  Ma (Figure 10B), and the sphalerite yields a model age of  $2,767 \pm 11.1$  Ma (Figure 10C).

Samples F013-001 (chalcopyrite), F013-002 (chalcopyrite), and F013-003 (chalcopyrite), collected from the sericite-chlorite zone, and samples F018-001b (sphalerite) and F018-002 (chalcopyrite), collected from the carbonate zone (massive sulfide), were used for isochron determination according to the Ludwig (2008) algorithm. The first isochron yielded a crystallization age of 2,753 Ma with a deviation of 210 Ma and a very high mean square weighted deviation (MSWD) of 68 (Figure 11A). However, using three points, samples F013-001 (chalcopyrite) and F013-003 (chalcopyrite) from the sericite-chlorite zone and sample F018-002 (chalcopyrite) from the carbonate zone, had isochron yielded age of  $2,747 \pm 16$  Ma with a deviation satisfactorily low and an ideal MSWD near one (Figure 11B). The age obtained using a greater diversity of samples, including sphalerite, is practically the same as the age obtained using three chalcopyrite samples; however, the last age obtained is more accurate. Therefore,  $2,747 \pm 16$  Ma is interpreted as the timing of mineralization.

The thorogenic ( $^{208}\text{Pb}$ – $^{206}\text{Pb}$ ) and uranium ( $^{207}\text{Pb}$ – $^{206}\text{Pb}$ ) diagrams follow the Zartman and Doe (1981) model, where the curves represent the tectonic settings of mantle, lower crust, upper crust, and orogen/mixture. In the thorogenic diagram (Figure 12A), the samples plot near the upper crust curve, but they are nearer the mantle and orogen curves, which are close together in this diagram. In the uranium diagram (Figure 12B), the samples are near the upper crust and orogen, but they move away from the mantle curve. Only two points are far from the set and near the mantle and lower crust curves.



Ccp: chalcopyrite; Gn: galena; Sp: sphalerite.

**Figure 9.** Drill cores used for Pb-Pb geochronological study of sulfides from the Fazenda Coqueiro volcanic-hosted massive sulfide deposit. (A) Carbonate zone with massive sphalerite from which four samples were obtained for the source study. (B) Silica-rich core level in the sericite-chlorite zone with galena sampled for model age study. (C, D, and E) Sericite-chlorite zone with disseminated chalcopyrite sampled for crystallization age and source study. (F) Carbonate-rich core with massive sphalerite from which two samples were obtained for model and crystallization ages and source study. (G) Carbonate zone core with chalcopyrite from which four samples (whole digestion and leached fractions) were obtained for model and crystallization ages and source study.

**Table 2.** Isotopic data for sulfide samples from the Fazenda Coqueiro volcanic-hosted massive sulfide deposit used for geochronological study.

Sample	Mineral analyzed	Host rock	Preparation technique	$^{206}\text{Pb}/^{204}\text{Pb}$	$2\sigma$	$^{207}\text{Pb}/^{204}\text{Pb}$	$2\sigma$	$^{208}\text{Pb}/^{204}\text{Pb}$	$2\sigma$
F006-12a	Sp	Carbonate zone	Whole digestion	13.884	0.002	14.855	0.002	33.662	0.006
F006-12b	Sp	Carbonate zone	Whole digestion	13.783	0.001	14.825	0.001	33.547	0.003
F006-12c	Sp	Carbonate zone	Whole digestion	13.849	0.002	14.837	0.002	33.616	0.005
F006-12d	Sp	Carbonate zone	Whole digestion	13.766	0.002	14.824	0.002	33.528	0.005
F006-014	Gn	Silica-rich level	Galena analysis	13.742	0.002	14.816	0.002	33.495	0.010
F013-001	Ccp	Sericite-chlorite zone	Whole digestion	24.836	0.043	16.952	0.028	43.039	0.073
F013-002	Ccp	Sericite-chlorite zone	Whole digestion	17.143	0.044	15.355	0.040	36.853	0.100
F013-003	Ccp	Sericite-chlorite zone	Whole digestion	16.460	0.022	15.369	0.022	36.148	0.053
F018-001a	Sp	Carbonate zone	Whole digestion	36.809	0.028	17.220	0.013	36.941	0.027
F018-001b	Sp	Carbonate zone	Whole digestion	13.759	0.001	14.832	0.002	33.556	0.006
F018-002	Ccp	Carbonate zone	Whole digestion	13.819	0.001	14.856	0.001	33.614	0.004
F018-002-L1	Ccp	Carbonate zone	Leached fraction	13.814	0.001	14.905	0.002	33.749	0.004
F018-002-L2	Ccp	Carbonate zone	Leached fraction	13.798	0.003	14.883	0.003	33.684	0.008
F018-002-L3	Ccp	Carbonate zone	Leached fraction	13.842	0.004	14.951	0.004	33.885	0.009

Ccp: chalcopyrite; Gn: galena; Sp: sphalerite.

## DISCUSSION

The actinolite content in the metabasalt can be the product of augite replacement under greenschist facies conditions, as described by Hashimoto (1972) for actinolite occurrences in low-grade basic metamorphic rocks. The anhedral, elongated, and partially broken sulfide grains, concordant with the foliation, suggest the sulfides were already crystallized when the Rhyacian-Orosirian metamorphism took place and they did not undergo melting or remobilization processes during the greenschist-facies metamorphism and deformation.

The sericite and chlorite grains may represent the primary hydrothermal alteration minerals that normally precede the main mineralization on the ocean floor and which

were preserved from low-grade greenschist-facies metamorphism. However, with the rising of temperature during the metamorphic event, replacements from chlorite to biotite and possibly from clay minerals to andalusite and cordierite took place, constituting aluminous schists. The anhedral, elongated and broken chalcopyrite, pyrrhotite, and pyrite grains indicate they had brittle behavior under deformation conditions and the metamorphic temperature they were submitted to. Thus, the melting and consequent remobilizations of the sulfides were unlikely.

The calcite grains of the carbonate zone show polygonization and triple junction that indicate recrystallization processes (Vokes, 1969). The intergrowth relation between the calcite and sphalerite during the ocean floor hydrothermal process was preserved from later low-grade metamorphism,

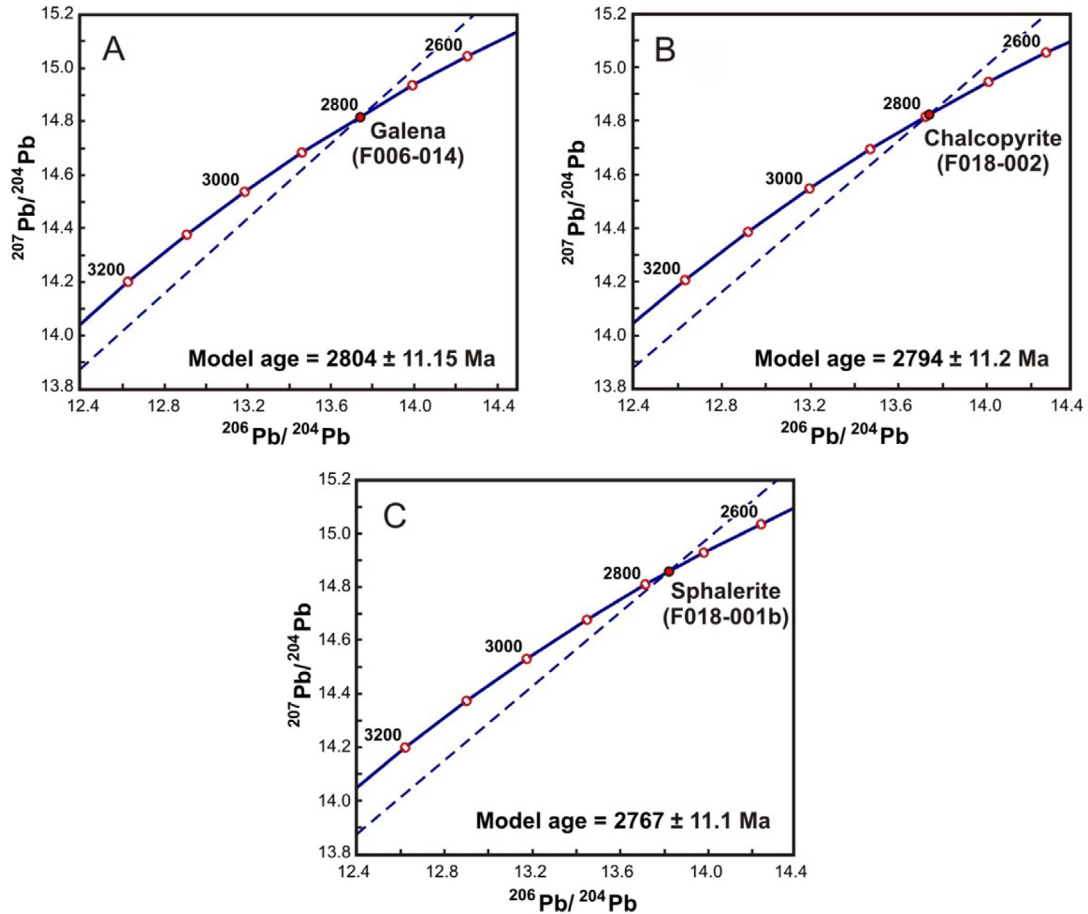


**Figure 10.**  $^{206}\text{Pb}/^{204}\text{Pb}$  vs.  $^{207}\text{Pb}/^{204}\text{Pb}$  diagram for model age determination for three sulfide samples from the Fazenda Coqueiro volcanic-hosted massive sulfide deposit: (A) Galena sample from the silica-rich level in the sericite-chlorite zone. (B) Chalcopyrite sample from the carbonate and massive sulfide zone. (C) Sphalerite sample from the carbonate and massive sulfide zone.

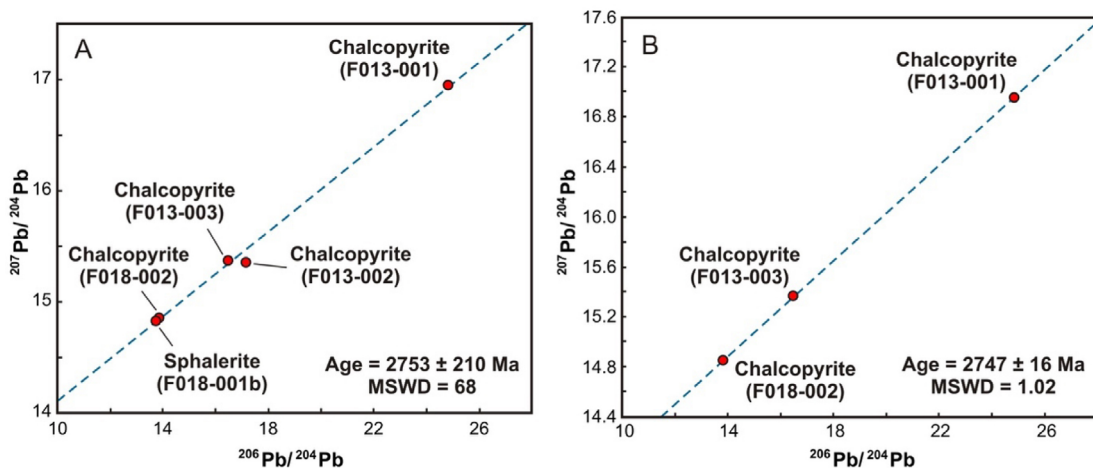


**Figure 11.** Detail of the isochron on the  $^{206}\text{Pb}/^{204}\text{Pb}$  vs.  $^{207}\text{Pb}/^{204}\text{Pb}$  diagram to determine the crystallization age of sulfides from the Fazenda Coqueiro volcanic-hosted massive sulfide deposit (MSWD). (A) Detailed isochron using five sulfide samples yields an age of  $2,753 \pm 210$  Ma with, however, a high MSWD of 68. (B) Detailed isochron using one sample of chalcopyrite from the massive sulfide zone (F018-002) and two samples of chalcopyrite from the disseminated sulfide zone in the sericite-chlorite zone (F013-001 and F013-003) that yields an age of  $2,747 \pm 16$  Ma and MSWD of 1.02.

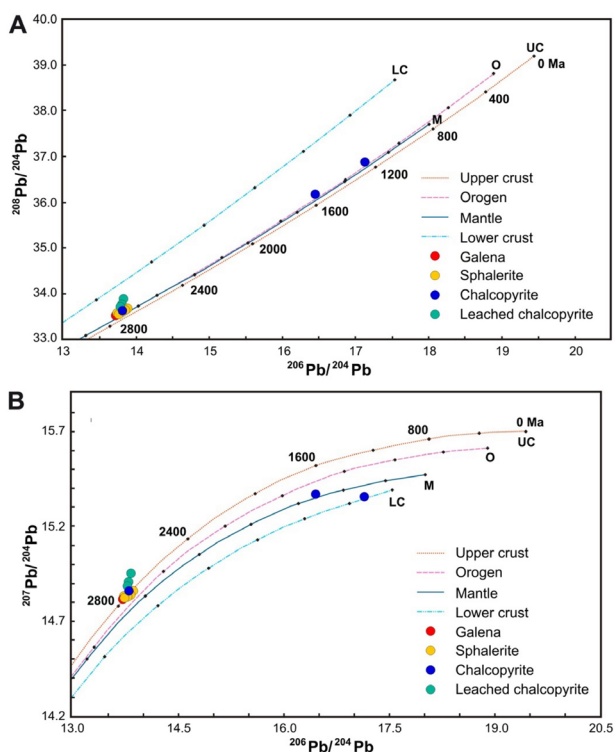


**Figure 12.** (A) Thorogenic and (B) uranogenic diagrams (Zartman and Doe, 1981) used for source study of the sphalerite, galena and chalcopyrite samples from the Fazenda Coqueiro volcanic-hosted massive sulfide deposit.

deformation and possible related hydrothermal processes. The paragenesis in VHMS deposits composed of sphalerite, galena, chalcopyrite, pyrrhotite, and pyrite and lacking sulfosalt and telluride minerals, have a melting temperature of approximately 730°C at 2MPa (Stevens et al., 2005; Tomkins et al., 2007). This temperature is considerably higher than the greenschist temperature in which the Fazenda Coqueiro rocks were submitted, which has a maximum temperature of approximately 450°C, according to Spear (1993), and that did not likely affect the sulfide paragenesis.

Although the calcite grains have no orientation, they were recrystallized and the massive sulfide lens related to them probably acted as a resistant body during the deformation processes of the Rhyacian-Orosirian tectonic event. The result was a translation displacement during the folding processes without development of foliation or mineral orientation, preserving thus the primary texture. The tectonic stress was concentrated in the contact of the massive sulfide body in the carbonate zone with the hanging and footwall rocks, where schistosity features were developed in the sericite-chlorite zone and in the western metabasalt.

The Pb-Pb analyses in sphalerite of the samples F006-12a, F006-12b, F006-12c, and F006-12d from the carbonate zone, each with a different mass, yield isotopic results that are close but not exactly the same, such as the different isotopic values for sphalerite from samples F018-001a and F018-001b, also from the carbonate zone. These results indicate that the sphalerite grains analyzed from the massive sulfide lens, hosted in the carbonate zone, show inclusions or blends with other minerals.

The similarity among the model ages of galena from the silica-rich level in the sericite-chlorite zone, and chalcopyrite and sphalerite from the carbonate zone —  $2,804 \pm 11.15$ ,  $2,794 \pm 11.2$ , and  $2,767 \pm 11.1$  Ma, respectively —, and the isochron age of  $2,747 \pm 16$  Ma, from disseminated and massive sulfides, suggest coherence in the data set indicating an initial isotopic homogeneity and a common evolutionary history until the formation of the sulfides. The high errors of the model ages take into consideration Pb evolution in the Earth according to the Stacey and Kramers (1975) model, which is certainly not obeyed in all geological cases. Nevertheless, the model ages indicate the moment that Pb was separated from the terrestrial reservoir to form the analyzed minerals.

The crystallization age of  $2,747 \pm 16$  Ma from the sulfides in the Fazenda Coqueiro VHMS deposit matches with one of the periods of VHMS deposit formation, which extended between 2.8 and 2.69 Ga, presented by Galley et al. (2007), which also presented other periods of VHMS formation in the Proterozoic and Phanerozoic eons. However, marked differences between the ancient VHMS deposits, such as that of the Fazenda Coqueiro, and those of modern VHMS types can be mentioned, as for example, the predominance of basalt-dominated volcanism in ancient deposits rather than andesitic or rhyolitic in the modern types (Gibson et al., 1997).

Regarding the source of the metals in the Fazenda Coqueiro deposit, contributions from the upper crust may have played an important role according the thorogenic and uranogenic diagrams for the Pb element that composes the sulfides. Therefore, the metals were probably transported during volcanism from the upper crust to their distribution and precipitation in the ocean floor setting, as proposed for the formation of the Fazenda Coqueiro deposit. The Zn solubility related primarily to pH variation and the Cu precipitation correlated with temperature, as discussed in Franklin et al. (2005), may explain the Zn concentration in the carbonate zone on the ocean floor and the spreading of Cu at the mineralization site. The Cu content is usually moderate in both proximal and distal zones; however, its values are highlighted in the sericite-chlorite zone due to the much lower Zn and Pb content in relation to the Cu content throughout this distal zone.

Submarine eruptions as that of the Fazenda Coqueiro VHMS deposit produced gases made up essentially of  $H_2S$  and  $CO_2$  from high pressure settings at great depths during the early Neoproterozoic and influenced the depth seawater content at that time, as shown by Gaillard et al. (2011). However, high pressure and great depths eruptions could not influence the atmosphere content, which would only be influenced by gas species stable near seawater surface, such as  $SO_2$  and  $H_2O$ , sourced from subaerial eruptions that existed only from the late Neoproterozoic (Kump and Barley, 2007), different from the scenario in the early Neoproterozoic, when the Fazenda Coqueiro VHMS deposit was formed.

The isochronic crystallization age of the sulfides hosted in the western metabasalt and correlated hydrothermal alteration zones of the Fazenda Coqueiro deposit obtained in this work of 2,747 Ma and the zircon crystallization age of 2,595 Ma obtained by Spreafico et al. (2019) from a meta-dacite occurrence in the central-north portion of the MNGB, both in the middle sequence, show Neoproterozoic records not previously described for this study area.

The geological and geochronological data presented suggest a coeval paragenesis for sulfides in both the massive and disseminated mineralized zones of the Fazenda Coqueiro deposit. The genesis of the western metabasalt and sericite-chlorite and the carbonate alteration zones seem to be related to the same ocean floor volcanic and hydrothermal event in the early Neoproterozoic (Figure 13A). Moreover, melting and remobilization of sulfides during the Rhyacian-Orosirian tectonic event are not supported by the present data that show that the Pb-Pb system on Fazenda Coqueiro sulfides was not affected by this tectono-thermal event.

Therefore, the greenschist-facies metamorphism observed in the Fazenda Coqueiro deposit rocks was not enough to destabilize the sphalerite, galena, chalcopyrite, pyrrhotite, and pyrite grains. In addition, the absence of elongated, stretched, and oriented grains in the massive sulfide lens suggests that it behaved as a competent rock during the Rhyacian-Orosirian tectonic event, preserving it from deformation processes. However, a translational transport during the folding processes positioned the sulfide lens in the eastern limb of the antiform observed in the Fazenda Coqueiro deposit as schematically shown in Figure 13B.

With regard to a more regional context, the Fazenda Coqueiro deposit would have formed in a Neoproterozoic oceanic crust, most likely in an arc-basin system (Spreafico et al., 2019), developed between the Gavião and Mairi blocks (Figure 14A). Finally, the oceanic crust was compressed during the west vergent Rhyacian-Orosirian tectonic event that imbricated the Fazenda Coqueiro deposit and the basement rocks (Figure 14B). This event was coeval to the formation of the Contendas-Jacobina lineament, within which the Fazenda Coqueiro deposit lies and when the area reached tectonic stability.

Hitherto, no other VHMS deposit has been described in the MNGB. However, Neoproterozoic oceanic crust occurrences along extensive regional lineaments, in addition to ocean floor hydrothermal alteration zones, such as carbonate, sericite-chlorite or silica-rich rocks, all of them related to basaltic rocks, can be used as prospecting guides for the discovery of other VHMS deposits in the eastern São Francisco Craton.

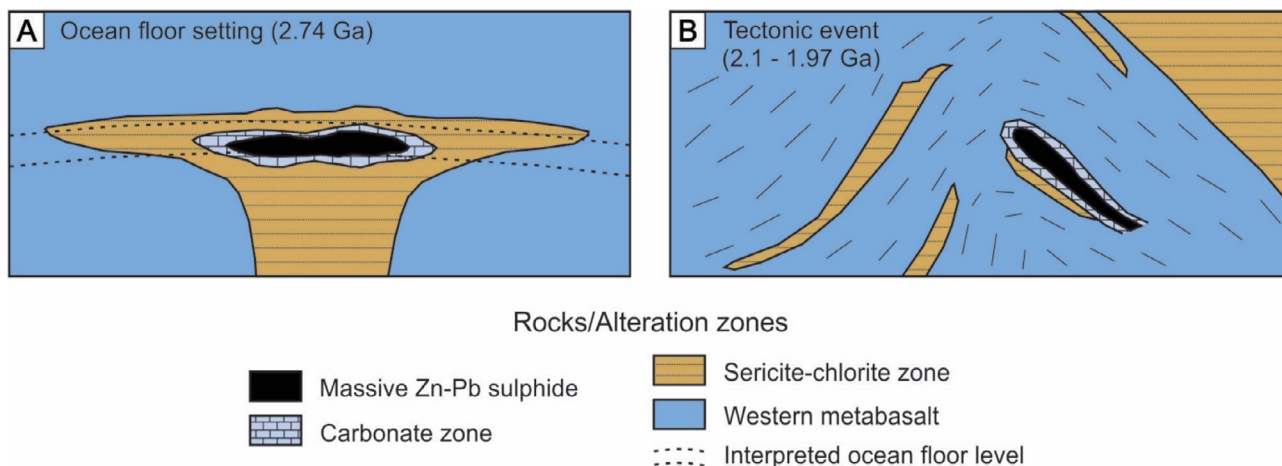


**Figure 13.** Metallogenic model of the Fazenda Coqueiro volcanic-hosted massive sulfide deposit. (A) Interpreted distribution and relation among the volcanic rock, massive sulfide and hydrothermal alteration zones in the ocean floor setting at 2,747 Ma. (B) Positioning of the massive sulfide lens and alteration zones after the Rhyacian-Orosirian tectonic event.

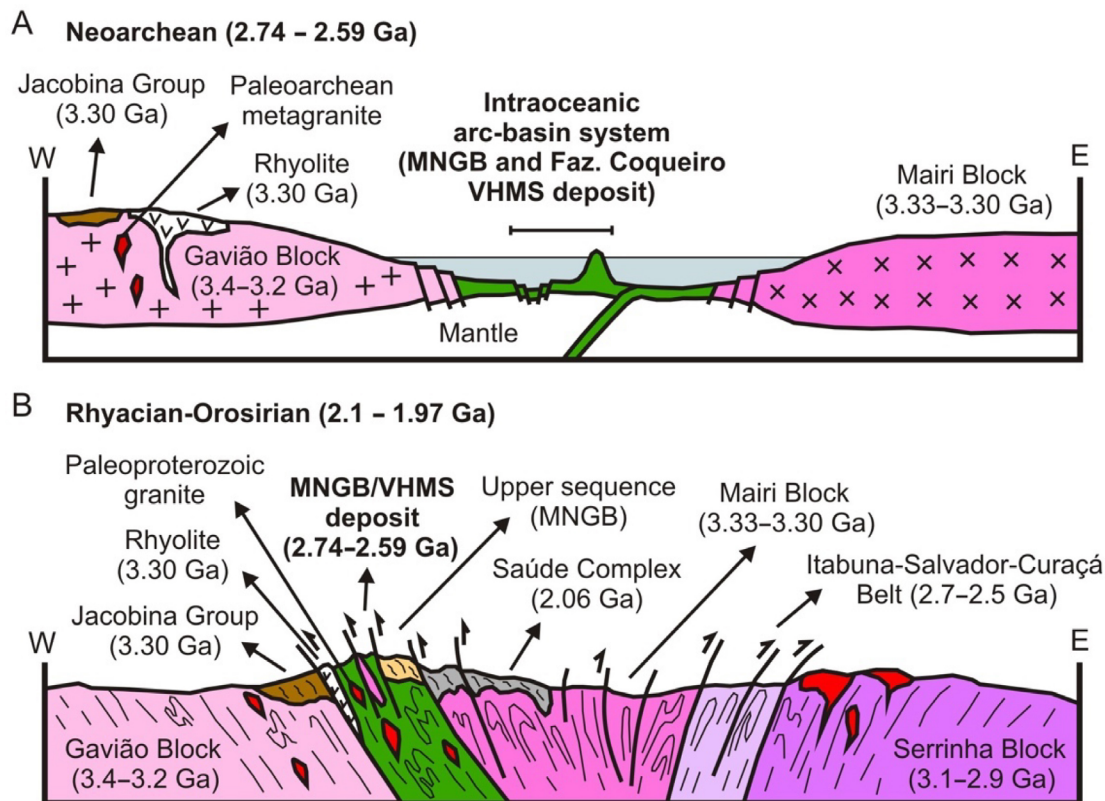


**Figure 14.** Regional geological setting of the Mundo Novo greenstone belt (MNGB) and Fazenda Coqueiro volcanic-hosted massive sulfide deposit. (A) Deposit formation in an intraoceanic arc-basin system at 2,747 Ma. (B) Final result of the Rhyacian-Orosirian tectonic event that compressed the MNGB and the Fazenda Coqueiro deposit between cratonic blocks in the eastern São Francisco Craton.

## CONCLUSIONS

The Zn-Pb-rich massive sulfide lens of the Fazenda Coqueiro VHMS deposit is strata-bound and related to the metamorphosed carbonate hydrothermal alteration zone, which is interlayered with the western metabasalt previously formed in an intraoceanic setting in the MNGB. The Cu-rich disseminated sulfide levels are related to the metamorphosed sericite-chlorite hydrothermal alteration zone, which is also interlayered with the western metabasalt.

The Pb in galena, chalcopyrite and sphalerite was sourced from the upper crust between 2,804 and 2,767 Ma, and the sulfides crystallized at 2,747 Ma during volcanic processes in the ocean floor setting, thus indicating the timing of mineralization. Therefore, we suggest that the Zn-Pb massive sulfide precipitated coeval to the hydrothermal carbonate that behaved as a chemical trap in the volcanic and hydrothermal system. The crystallization of the chalcopyrite was related to the sericite and chlorite in the initial stage of the hydrothermal process.

We also interpret that the temperature reached by greenschist-facies metamorphism during the Rhyacian-Orosirian

period was not enough to melt or remobilize the sulfides, and therefore did not affect the Pb-Pb isotopic system. The massive sulfide lens and the related carbonate zone acted as a resistant body during the Rhyacian-Orosirian tectonic event preserving the primary textures.

The Rhyacian-Orosirian tectonic event compressed the Fazenda Coqueiro deposit between Archean cratonic blocks along the Contendas-Jacobina lineament. Therefore, occurrences of oceanic crust along extensive regional lineaments with evidence of ocean floor hydrothermal activities are good prospecting guides for VHMS-type deposits in the eastern portion of the São Francisco Craton.

## ACKNOWLEDGMENTS

This research was linked to the PhD program of the *Instituto de Geociências, Universidade Federal da Bahia*, and was financially supported by the *Companhia Baiana de Pesquisa Mineral* and, partly, by the *Coordenação de Aperfeiçoamento de Pessoal de Nível Superior (CAPES)*—Funding Code 001.

## REFERENCES

- Barbosa, J. S. F. (1997). Síntese do Conhecimento sobre a Evolução Geotectônica das Rochas Metamórficas Arqueanas e Paleoproterozóicas do Embasamento do Cráton do São Francisco na Bahia. *Revista Brasileira de Geociências*, 27(3), 241-256. <https://doi.org/10.25249/0375-7536.1997241256>
- Barbosa, J. S. F., Cruz, S. C. P., Souza, J. S. (2012a). Terrenos metamórficos do embasamento. In: J. S. F. Barbosa (Ed.), *Geologia da Bahia: Pesquisa e Atualização* (v. 1, p. 101-201). Salvador: CBPM. Available at: <<http://www.cbpm.ba.gov.br/book/geologia-da-bahia-pesquisa-e-atualizacao/>>. Accessed on: July 22, 2020.
- Barbosa, J. S. F., Pinto, M. S., Cruz, S. C. P., Souza, J. S. (2012b). Granitoides. In: J. S. F. Barbosa (Ed.), *Geologia da Bahia: Pesquisa e Atualização* (v. 1, p. 327-396). Salvador: CBPM. Available at: <<http://www.cbpm.ba.gov.br/book/geologia-da-bahia-pesquisa-e-atualizacao/>>. Accessed on: July 22, 2020.
- Barbosa, J. S. F., Sabaté, P. (2002). Geological features and the Paleoproterozoic collision of four Archean crustal segments of the São Francisco Craton, Bahia, Brazil. A synthesis. *Anais da Academia Brasileira de Ciências*, Rio de Janeiro, 74(2), 343-359. <https://doi.org/10.1590/S0001-37652002000200009>
- Barbosa, J. S. F., Sabaté, P. (2003). Colagem paleoproterozoica de placas arqueanas do Cráton do São Francisco na Bahia. *Revista Brasileira de Geociências*, 33(Supl. 1), 7-14. <https://doi.org/10.25249/0375-7536.200333S10714>
- Barbosa, J. S. F., Sabaté, P. (2004). Archean and Paleoproterozoic crust of the São Francisco Craton, Bahia, Brazil: geodynamic features. *Precambrian Research*, 133(1-2), 1-27. <https://doi.org/10.1016/j.precamres.2004.03.001>
- Barbuena, D., Oliveira, E. P., Zincone, S. A. (2016). Estudos de proveniência dos quartzitos do Greenstone Belt Mundo Novo (BA) e implicações tectono-estratigráficas. *XLVIII Congresso Brasileiro de Geologia*. Porto Alegre: SBG. p. 818. Available at: <<http://cbg2017anais.siteoficial.ws/anais48cbgcompleto.pdf>>. Accessed on: July 22, 2020.
- Couto, P. A., Sampaio, A. R., Gil, C. A. A., Loureiro, H. C., Arcanjo, J. B., Fernandes Filho, J., Guimarães, J. T., Campelo, R., Mascarenhas, J. F., Bruni, D. C., Toledo, L. A. A. (1978). *Projeto Serra de Jacobina: Geologia e Prospecção Geoquímica*. Salvador: DNPM-CPRM. Available at: <<http://rigeo.cprm.gov.br/jspui/handle/doc/9602>>. Accessed on: July 22, 2020.
- Franklin, J. M., Gibson, H. L., Jonasson, I. R., Galley, A. G. (2005). Volcanogenic Massive Sulfide Deposits. In: J. W. Hedenquist, J. F. H. Thompson, R. J. Goldfarb, J. P. Richards (Eds.), *Economic Geology*, 100<sup>th</sup> anniversary volume, p. 523-560. <https://doi.org/10.5382/AV100.17>
- Gaillard, F., Scaillet, B., Arndt, N. T. (2011). Atmospheric oxygenation caused by a change in volcanic degassing pressure. *Nature*, 478, 229-232. <https://doi.org/10.1038/nature10460>
- Galley, A. G., Hannington, M. D., Jonasson, I. R. (2007). Volcanogenic massive sulfide deposits. In: W. D. Goodfellow (Ed.), *Mineral deposits of Canada: A Synthesis of Major Deposit-Types, District Metallogeny, the Evolution of Geological Provinces, and Exploration Methods* (v. 5, p. 141-161). Ottawa: Geological Association of Canada.
- Gibson, H. L., Morton, R. L., Hudak, G. J. (1997). Submarine Volcanic Processes, Deposits, and Environments Favorable for the Location of Volcanic-Associated Massive Sulfide Deposits. In: C. T. Barrie, M. D. Hannington (Eds.), *Volcanic Associated Massive Sulfide Deposits: Processes and Examples in Modern and Ancient Settings* (p. 13-51). Ottawa: Geological Survey of Canada. (Reviews in Economic Geology, 8.)
- Hashimoto, M. (1972). Reactions producing actinolite in basic metamorphic rocks. *Lithos*, 5(1), 19-31. [https://doi.org/10.1016/0024-4937\(72\)90077-1](https://doi.org/10.1016/0024-4937(72)90077-1)
- Kretz, R. (1983). Symbols for rock-forming minerals. *American Mineralogist*, 68(1), 277-279. Available at: <[https://www.researchgate.net/publication/216831138\\_Symbols\\_for\\_rock-forming\\_minerals](https://www.researchgate.net/publication/216831138_Symbols_for_rock-forming_minerals)>. Accessed on: July 22, 2020.
- Kump, L. R., Barley, M. E. (2007). Increased subaerial volcanism and the rise of atmospheric oxygen 2.5 billion years ago. *Nature*, 448, 1033-1036. <https://doi.org/10.1038/nature06058>
- Leal, L. R. B. (1998). *Geocronologia U/Pb (SHRIMP), 207Pb/206Pb, Rb/Sr, Sm/Nd e K/Ar dos Terrenos Granito-Greenstone do Bloco do Gavião: Implicações para a Evolução Arqueana e Paleoproterozoica do Cráton do São Francisco, Brasil*. Thesis (Doctoring). São Paulo: Universidade de São Paulo. <https://doi.org/10.11606/T.44.2016.tde-08012016-145912>
- Leite, C. M. M. (2002). *A Evolução Geodinâmica da Orogênese Paleoproterozóica nas Regiões de Capim Grosso, Jacobina e Pintadas - Mundo Novo (Bahia-Brasil): Metamorfismo, Anatexia Crustal e Tectônica*. Thesis (Doctoring). Salvador: Instituto de Geociências - UFBA.

- Leite, C. M. M., Barbosa, J. S. F., Nicollet, C., Sabaté, P. (2007). Evolução metamórfica/metassomática paleoproterozóica do Complexo Saúde, da Bacia Jacobina e de leucogranitos peraluminosos na parte norte do Cráton do São Francisco. *Revista Brasileira de Geociências*, 37(4), 777-797. <https://doi.org/10.25249/0375-7536.200737477797>
- Ludwig, K. R. (2008). User's manual for ISOPLOT/EX: a geochronological toolkit for Microsoft Excel (version 3.68). Special Publication. Berkeley: Berkeley Geochronology Center.
- Magee, C. W., Palin, J. M., Taylor, W. R. (2001). Laser ICP-MS U/Pb analyses of detrital zircons from Proterozoic sediments in Bahia state, Brazil; implications for the evolution of the São Francisco craton prior to 3.3 Ga. *XI V.M. Goldschmidt Conference*, 3501. Hot Springs - Geochemical Society. Available at: <<https://www.lpi.usra.edu/meetings/gold2001/pdf/3501.pdf>>. Accessed on: July 22, 2020.
- Mascarenhas, J. F., Ledru, P., Souza, S. L., Filho, V. M. C., Melo, L. F. A., Lorenzo, C. L., Milesi, J. P. (1998). Geologia e recursos minerais do Grupo Jacobina e da parte sul do Greenstone Belt de Mundo Novo. *Série Arquivos Abertos (CBPM)*, 13, 1-58. Available at: <<http://www.cbpm.ba.gov.br/book/geologia-e-recursos-minerais-do-grupo-jacobina-e-da-parte-sul-do-greenstone-belt/>>. Accessed on: July 22, 2020.
- Monteiro, M. D., Silva, R. W. S., Cunha, J. C. (2009). *Projeto Fazenda Coqueiro*. Salvador: CBPM.
- Mougeot, R. (1996). *Etude de la limite Archéen-Protérozoïque et des minéralisations Au, +U associées: exemples des régions de Jacobina (Etat de Bahia, Brésil) et de Carajas (Etat de Para, Brésil)*. Thesis (Doctoring). Montpellier: Université de Montpellier II. Available at: <<http://www.theses.fr/1996MON20131>>. Accessed on: July 22, 2020.
- Oliveira, E. P., McNaughton, N. J., Armstrong, R. (2010). Mesoarchean to Paleoproterozoic growth of the northern segment of the Itabuna-Salvador-Curaçá orogeny, São Francisco Cráton, Brazil. In: T. M. Kusky, M. G. Zhai, W. Xiao (Eds.), *The evolving continents: understanding processes of continental growth* (v. 338, p. 263-286). London: Geological Society Special Publication.
- Oliveira, E. P., Mello, E. F., McNaughton, N. (2002a). Reconnaissance U-Pb geochronology of Precambrian quartzites from the Caldeirão belt and their basement, NE São Francisco Craton, Bahia, Brazil: implications for the early evolution of the Paleoproterozoic Itabuna-Salvador-Curaçá orogeny. *Journal of South American Earth Sciences*, 15(3), 349-362. [https://doi.org/10.1016/S0895-9811\(02\)00039-1](https://doi.org/10.1016/S0895-9811(02)00039-1)
- Oliveira, E. P., Mello, E. F., McNaughton, N. J., Choudhuri, A. (2002b). SHRIMP U-Pb age of the basement to the Rio Itapicuru Greenstone Belt, NE São Francisco craton. *XLII Congresso Brasileiro de Geologia*. João Pessoa: SBG. p. 522.
- Peucat, J. J., Mascarenhas, J. F., Barbosa, J. S. F., Souza, S. L., Marinho, M. M., Fanning, C. M., Leite, C. M. M. (2002). 3,3 Ga SHRIMP U-Pb zircon age of a felsic metavolcanic rock from the Mundo Novo Greenstone Belt in the São Francisco Craton, Bahia (NE Brazil). *Journal of South American Earth Sciences*, 15(3), 363-373. [https://doi.org/10.1016/S0895-9811\(02\)00044-5](https://doi.org/10.1016/S0895-9811(02)00044-5)
- Reis, C., Menezes, R. C. L., Miranda, D. A., Santos, F. P., Loureiro, H. C., Neves, J. P., Viera, R. (2017). *Mapa geológico-geofísico: Projeto ARIM Serra de Jacobina*. Salvador: CPRM. Available at: <<http://rigeo.cprm.gov.br/jspui/handle/doc/18679>>. Accessed on: July 22, 2020.
- Reis, C., Oliveira, R. C. L., Miranda, D. A., Santos, F. P., Guimarães, J. T., Teles, G. (2018). Estratigrafia do grupo Jacobina. *XLIX Congresso Brasileiro de Geologia*. Rio de Janeiro: SBG. p. 1232. Available at: <<http://cbg2018anais.siteoficial.ws/resumos/7641.pdf>>. Accessed on: July 22, 2020.
- Rios, D. C., Davis, D. W., Conceição, H., Davis, W. J., Rosa, M. L. S., Dickin, A. P. (2009). Geologic evolution of the Serrinha nucleus granite-greenstone terrane (NE Bahia, Brazil) constrained by U-Pb single zircon geochronology. *Precambrian Research*, 170(3-4), 175-201. <https://doi.org/10.1016/j.precamres.2008.10.001>
- Siivola, J., Schmid, R. (2007). *A systematic nomenclature for metamorphic rocks*. List of mineral abbreviations. Recommendations by the IUGS Subcommittee on the Systematics of Metamorphic Rocks. USA - IUGS. Available at: <<https://www.bgs.ac.uk/downloads/start.cfm?id=3197>>. Accessed on: July 22, 2020.
- Silva, L. C., Armstrong, R., Delgado, I. M., Pimentel, M., Arcanjo, J. B., Melo, R. C., Teixeira, L. R., Jost, H., Cardoso Filho, J. M., Pereira, L. H. M. (2002). Reavaliação da evolução geológica em terrenos Pré-Cambrianos brasileiros com base em novos dados U-Pb SHRIMP, Parte I: Limite centro-oriental do Cráton São Francisco na Bahia. *Revista Brasileira de Geociências*, 32(4), 501-512. <https://doi.org/10.25249/0375-7536.2002324501512>
- Silva, L. C., McNaughton, N. J., Melo, R. C., Fletcher, I. R. (1997). U-Pb SHRIMP ages in the Itabuna-Caraíba TTG high-grade complex: the first window beyond the Paleoproterozoic overprinting of the eastern Jequié Craton, NE Brazil. *International Symposium on Granites and Associated Mineralization*, 1, 282-283. Salvador. Available at: <<https://www.researchgate.net/publication/284106273>>. Accessed on: July 22, 2020.

- Sousa, D. F. M., Oliveira, E. P., Amaral, W. S. (2018). Geologia e geocronologia U-Pb em zircão de ortognaisses e K-granitoides relacionados ao Bloco Gavião (Complexo Mairi) e Cinturão Salvador-Curaçá – Região da Mina Caraíba – Bahia. *XLIX Congresso Brasileiro de Geologia*, 980. Rio de Janeiro: SBG. Available at: <<http://cbg2018anais.siteoficial.ws/resumos/8534.pdf>>. Accessed on: July 22, 2020.
- Souza, S. L., Garrido, I. A. A., Oliveira, N. S., Frões, R. J. (2002). *Projeto Greenstone Belt de Mundo Novo: estudos geológicos regionais*. Salvador: CBPM. v. 1. 62 p.
- Spear, F. S. (1993). *Metamorphic Phase Equilibria and Pressure-Temperature-Time Paths*. Mineralogical Society of America.
- Spreafico, R. R. (2017). *Projeto Mundo Novo: texto e mapas*. Salvador: CBPM.
- Spreafico, R. R., Barbosa, J. S. F., Barbosa, N. S., Moraes, A. M. V. (2019). Tectonic evolution of the Neoproterozoic Mundo Novo greenstone belt, eastern São Francisco Craton, NE Brazil: petrology, U-Pb geochronology, and Nd and Sr isotopic constraints. *Journal of South American Earth Sciences*, 95, 102296. <https://doi.org/10.1016/j.jsames.2019.102296>
- Stacey, J. S., Kramers, J. D. (1975). Approximation of terrestrial lead isotope evolution by a two stage model. *Earth and Planetary Science Letters*, 26(2), 207-221. [https://doi.org/10.1016/0012-821X\(75\)90088-6](https://doi.org/10.1016/0012-821X(75)90088-6)
- Stevens, G., Prinz, S., Rozendaal, A. (2005). Partial melting of the assemblage sphalerite + galena + pyrrhotite + chalcopyrite + sulfur: Implications for high-grade metamorphosed massive sulfide deposits. *Economic Geology*, 100(4), 781-786. <https://doi.org/10.2113/gsecongeo.100.4.781>
- Teles, G. S. (2013). *Proveniência e idades de deposição dos sedimentos auríferos da Bacia de Jacobina: Implicações sobre a evolução da bacia durante o Paleó-Arqueano e a gênese da mineralização*. Dissertation (Mastering). Brasília: Instituto de Geociências, Universidade de Brasília. Available at: <<http://repositorio.unb.br/handle/10482/14972>>. Accessed on: July 22, 2020.
- Teles, G. S., Chemale Jr., F., Oliveira, C. G. (2015). Paleoproterozoic record of the detrital pyrite-bearing, Jacobina Au-U deposits, Bahia, Brazil. *Precambrian Research*, 256, 289-313. <https://doi.org/10.1016/j.precamres.2014.11.004>
- Tomkins, A. G., Pattison, D. R. M., Frost, B. R. (2007). On the Initiation of Metamorphic Sulfide Anatexis. *Journal of Petrology*, 48(3), 511-535. <https://doi.org/10.1093/petrology/egl070>
- Vokes, F. M. (1969). A review of the metamorphism of sulphide deposits. *Earth-Science Reviews*, 5(2), 99-143. [https://doi.org/10.1016/0012-8252\(69\)90080-4](https://doi.org/10.1016/0012-8252(69)90080-4)
- Wilson, N. (1987). *Combined Sm-Nd, Pb-Pb and Rb-Sr geochronology and isotope geochemistry in polymetamorphic precambrian terrains: examples from Bahia, Brazil and Channel Island*. Dissertation (Master). Oxford: Oxford University.
- Zartman, R. E., Doe, B. R. (1981). Plumbotectonics - the model. *Tectonophysics*, 75(1-2), 135-162. [https://doi.org/10.1016/0040-1951\(81\)90213-4](https://doi.org/10.1016/0040-1951(81)90213-4)
- Zincone, S. A., Barbuena, D., Oliveira, E. P., Baldim, M. R. (2017). Detrital zircon U-Pb ages as evidence for deposition of the Saúde Complex in a Paleoproterozoic foreland basin, northern São Francisco Craton, Brazil. *Journal of South American Earth Sciences*, 79, 537-548. <https://doi.org/10.1016/j.jsames.2017.09.009>
- Zincone, S. A., Oliveira, E. P., Laurent, O., Zhang, H., Zhai, M. (2016). 3,3 Ga High-Silica Intraplate Volcanic-Plutonic System of the Gavião Block, São Francisco Craton, Brazil: Implications of an intracontinental rift following the creation of insulating continental crust. *Lithos*, 266-267, 414-434. <https://doi.org/10.1016/j.lithos.2016.10.011>

#### Appendix 1. Collar coordinates of the drill holes in Figure 8. Datum: SIRGAS 2000.

Drill hole	W. Long.	S. Lat.
FCQ-06	40° 29' 35.54"	11° 53' 35.25"
FCQ-13	40° 29' 24.71"	11° 53' 37.09"
FCQ-16	40° 29' 27.40"	11° 53' 33.15"
FCQ-18	40° 29' 37.04"	11° 53' 30.44"
FCQ-22	40° 29' 45.48"	11° 53' 34.57"

Long.: longitude; Lat.: latitude.